Systematic errors in GW parameter estimation

Hee-Suk Cho (Pusan National University)

66th GWNR workshop 2022.09.02

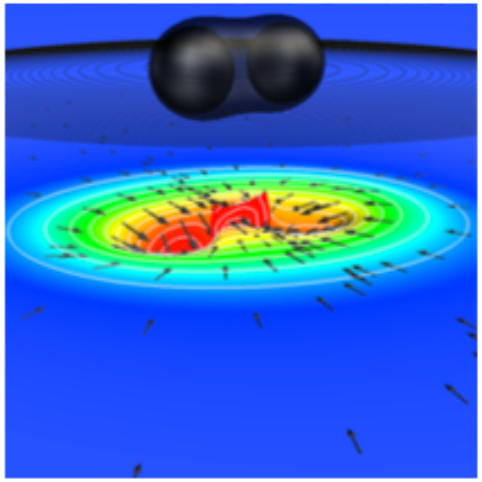

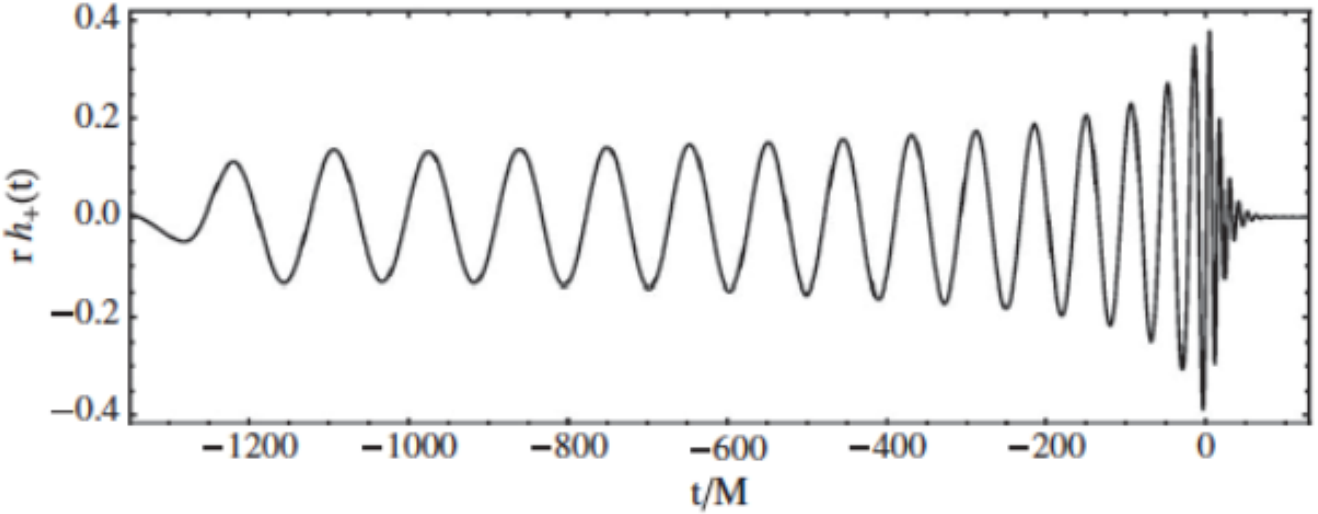

Outline

- Compact Binary Coalescence (CBC) waveforms
  - nonspinning
  - precessing (amplitude modulation)
  - PN phase evolution
  - waveform models
- CBC data analysis
  - matched filter
  - efficiency of template bank: fitting factor
  - detection & parameter estimation
- Systematic error in parameter estimation
  - examples
  - impact of eccentricity (review on recent works)

Gravitational-Wave Sources

$$\bar{h}_{ij}(t,r) = \frac{2G}{c^4 r}\ddot{I}_{ij}(t - r/c).$$

I_{ij} is the mass quadrupole moment.

very weak, accelerating objects, speed of light

Compact Binary Coalescences:
Neutron Stars / Black Holes

Burst sources: Supernovae
Large uncertainties on waveforms

Continuous sources: Pulsars

Stochastic background
from cosmological origin

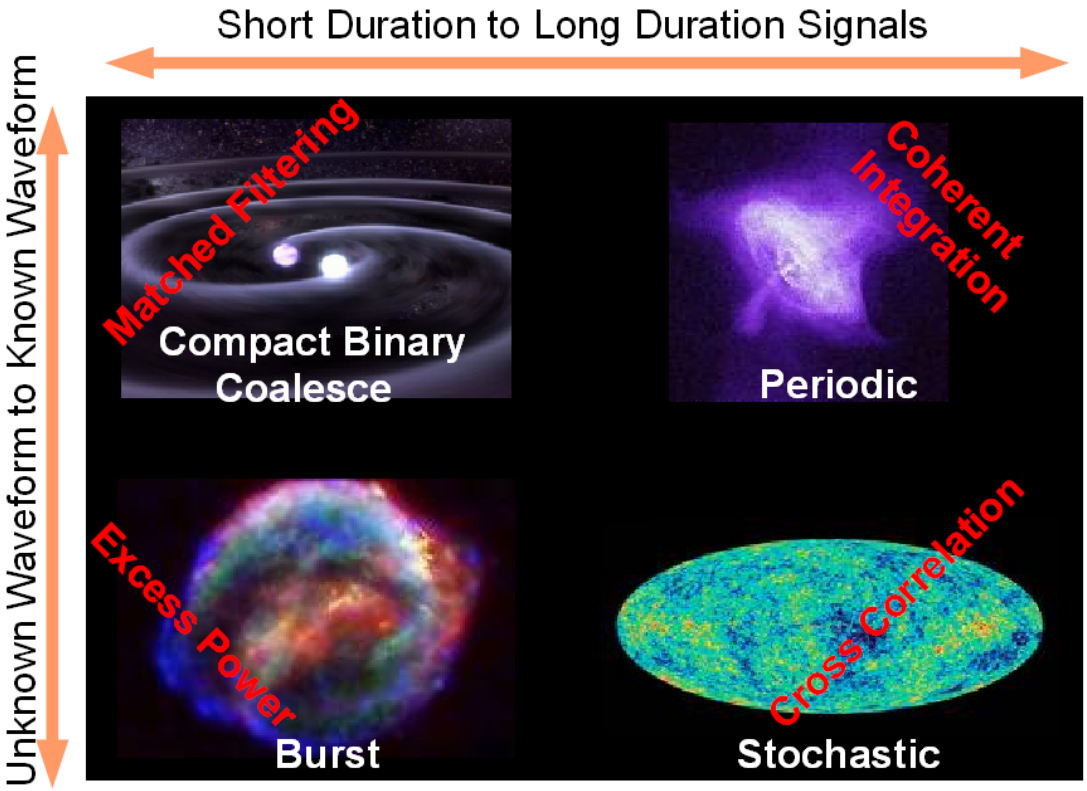

CBC GW polarization

$$h_+ = -\frac{2G\mu}{c^2 R} x(1+\cos^2\Theta)\cos 2\psi$$

$$h_\times = -\frac{2G\mu}{c^2 R} x(2\cos\Theta)\sin 2\psi$$

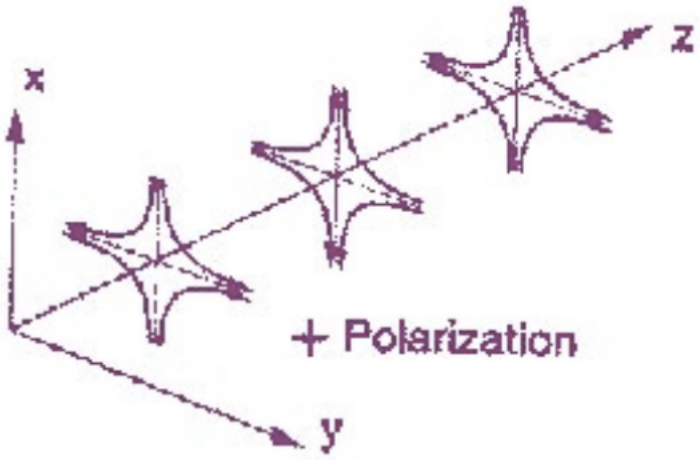

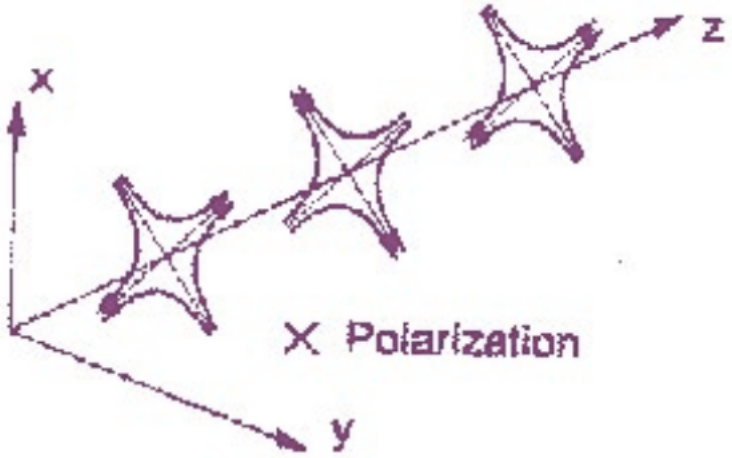

Radiation power

$$h_+ = -\frac{2G\mu}{c^2 R} x(1+\cos^2\Theta)\cos 2\psi$$
$$h_\times = -\frac{2G\mu}{c^2 R} x(2\cos\Theta)\sin 2\psi$$

$$\left(\frac{dP}{d\Omega}\right) = \frac{r^2 c^3}{16\pi G}\langle \dot{h}_+^2 + \dot{h}_\times^2 \rangle.$$

$$\left(\frac{dP}{d\Omega}\right) = \frac{2G\mu^2 a^4 \omega^6}{\pi c^5} g(\Theta),$$

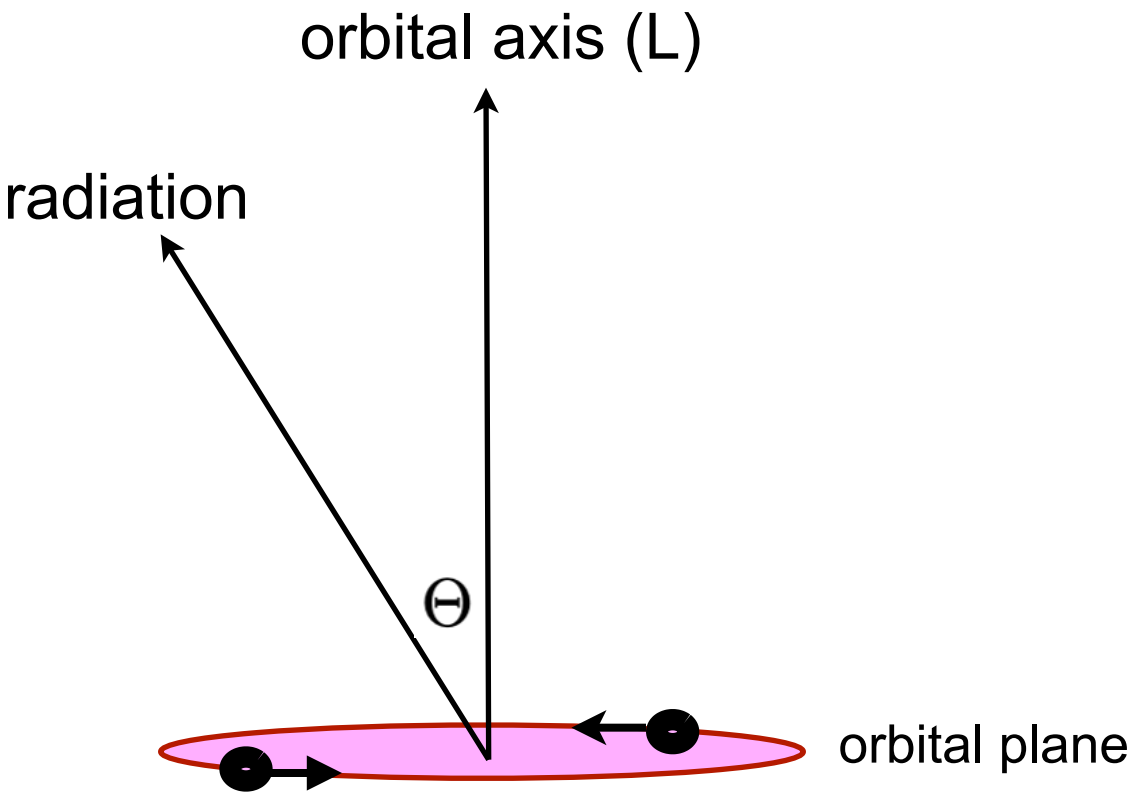

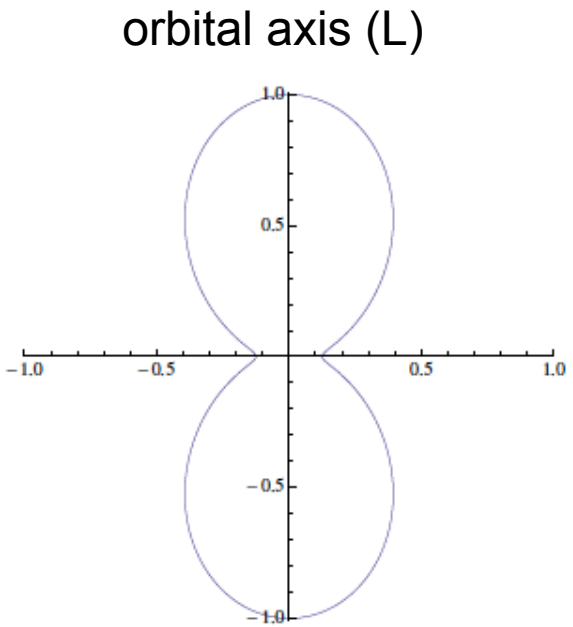

GW polarization: non spinning

$$h_+ = -\frac{2G\mu}{c^2 R} x (1 + \cos^2 \Theta) \cos 2\psi$$

$$h_\times = -\frac{2G\mu}{c^2 R} x (2 \cos \Theta) \sin 2\psi$$

Orbital phase

Inclination

PN parameter

$$x \equiv \left(\frac{G m \omega}{c^3}\right)^{2/3}$$

Waveform: non spinning

$$h_+ = -\frac{2G\mu}{c^2 R} x(1+\cos^2\iota)\cos 2\psi$$

$$h_\times = -\frac{2G\mu}{c^2 R} x(2\cos\iota)\sin 2\psi$$

Amplitude:monotonically increases

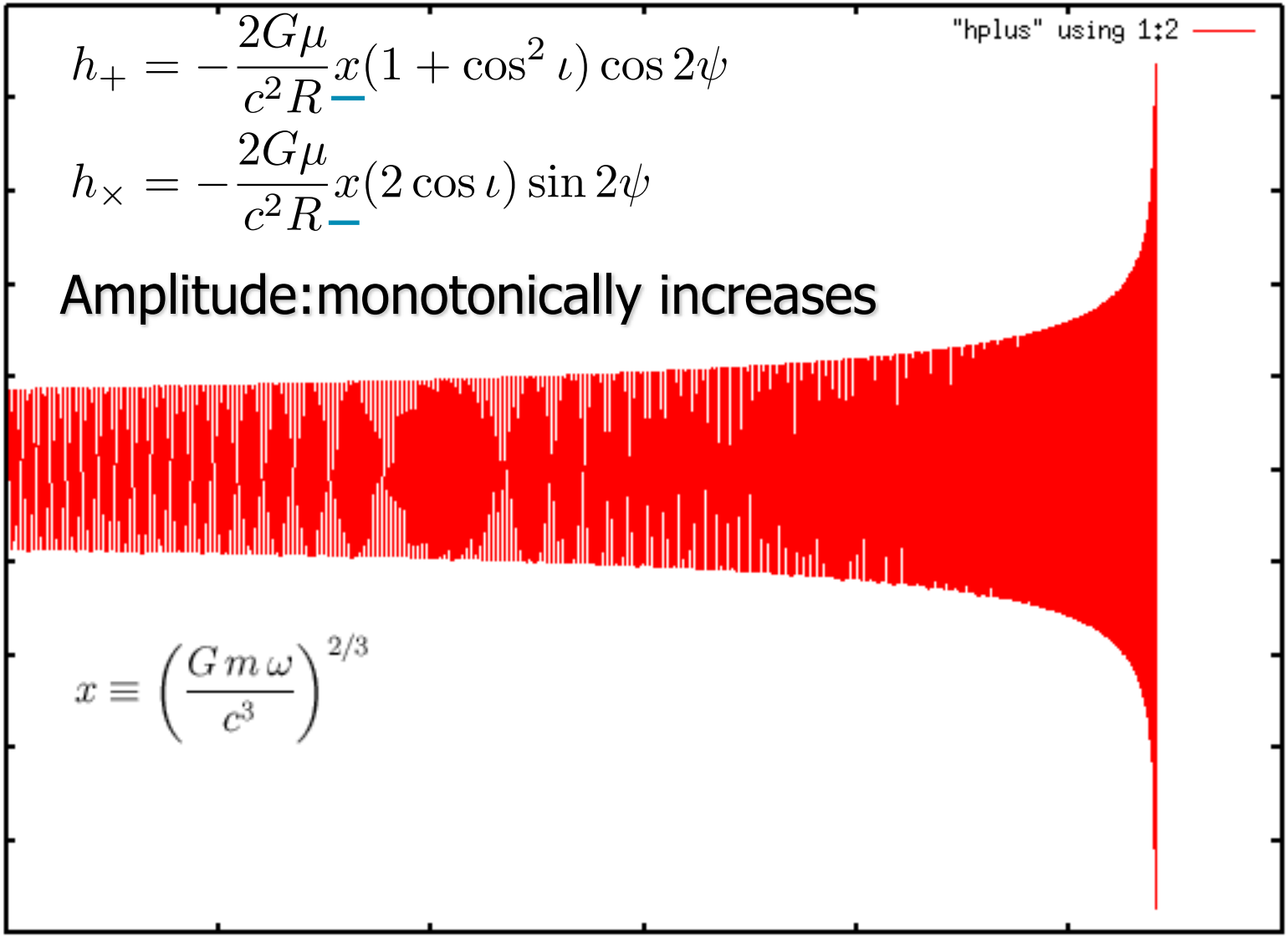

$$x \equiv \left(\frac{G\,m\,\omega}{c^3}\right)^{2/3}$$

Waveform: non spinning

$$h_+ = -\frac{2G\mu}{c^2 R} x(1+\cos^2\iota)\cos 2\psi$$

$$h_\times = -\frac{2G\mu}{c^2 R} x(2\cos\iota)\sin 2\psi$$

Amplitude:monotonically increases

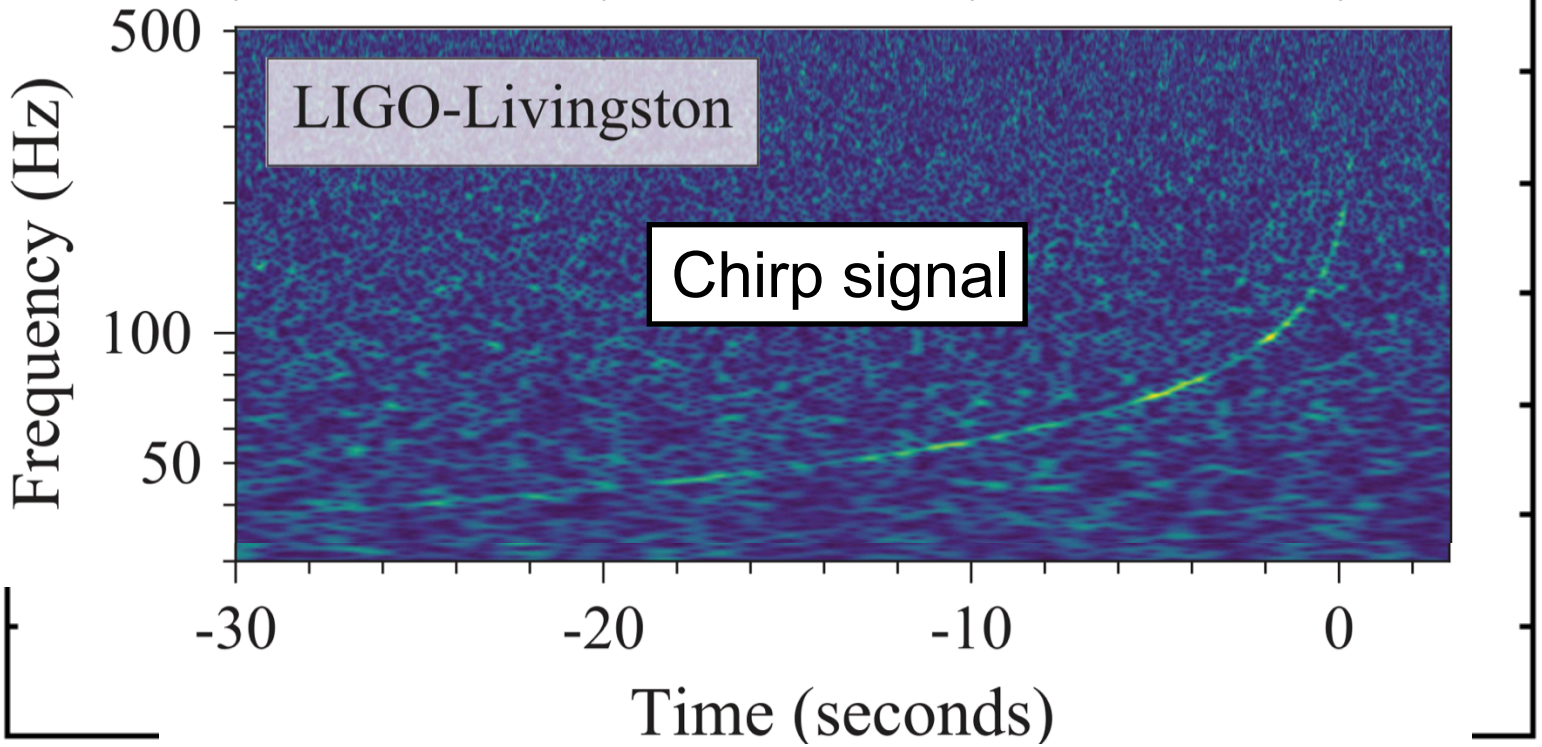

Inclination (Θ)

$$h_+ = -\frac{2G\mu}{c^2 R} x(1+\cos^2\Theta)\cos 2\psi$$

$$h_\times = -\frac{2G\mu}{c^2 R} x(2\cos\Theta)\sin 2\psi$$

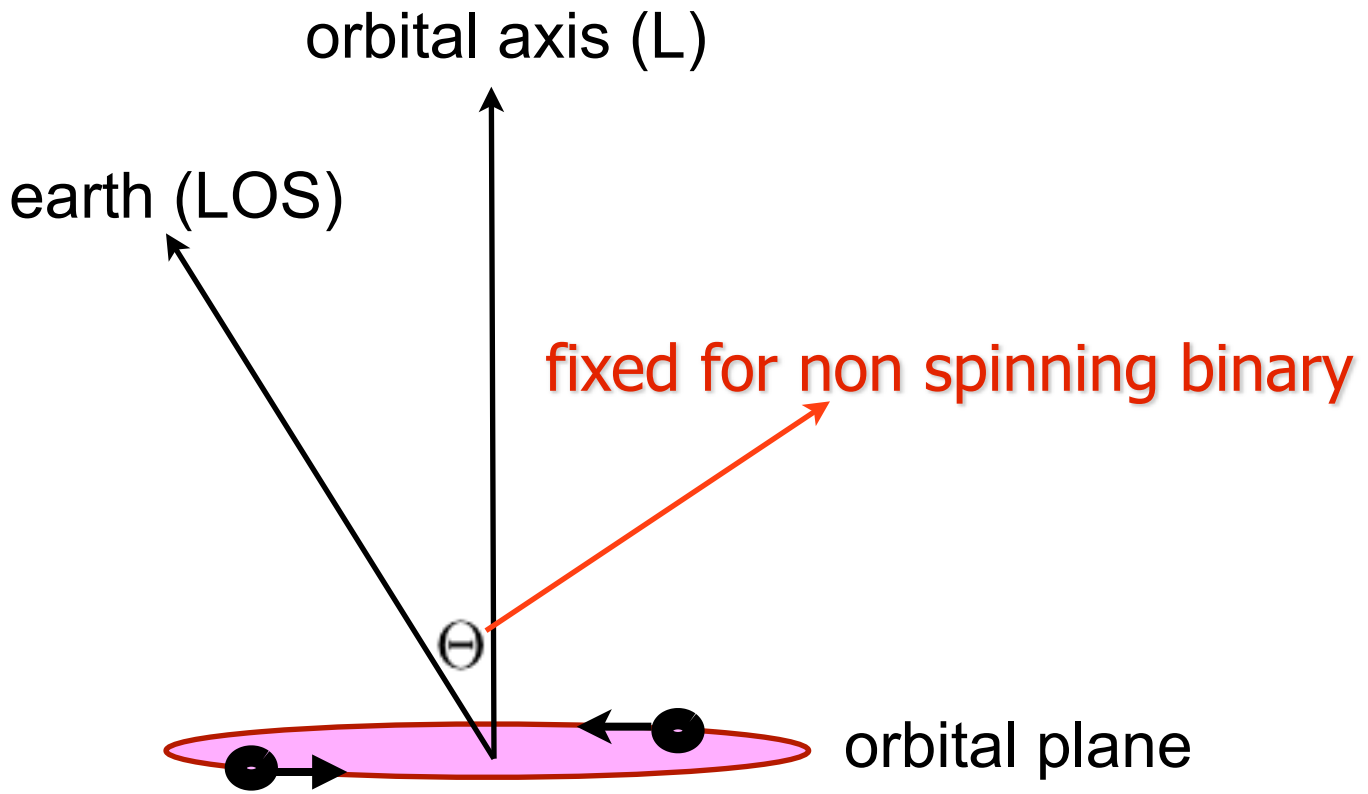

Dependence on inclination

$$h_+ = -\frac{2G\mu}{c^2 R} x(1+\cos^2\Theta)\cos 2\psi$$

$$h_\times = -\frac{2G\mu}{c^2 R} x(2\cos\Theta)\sin 2\psi$$

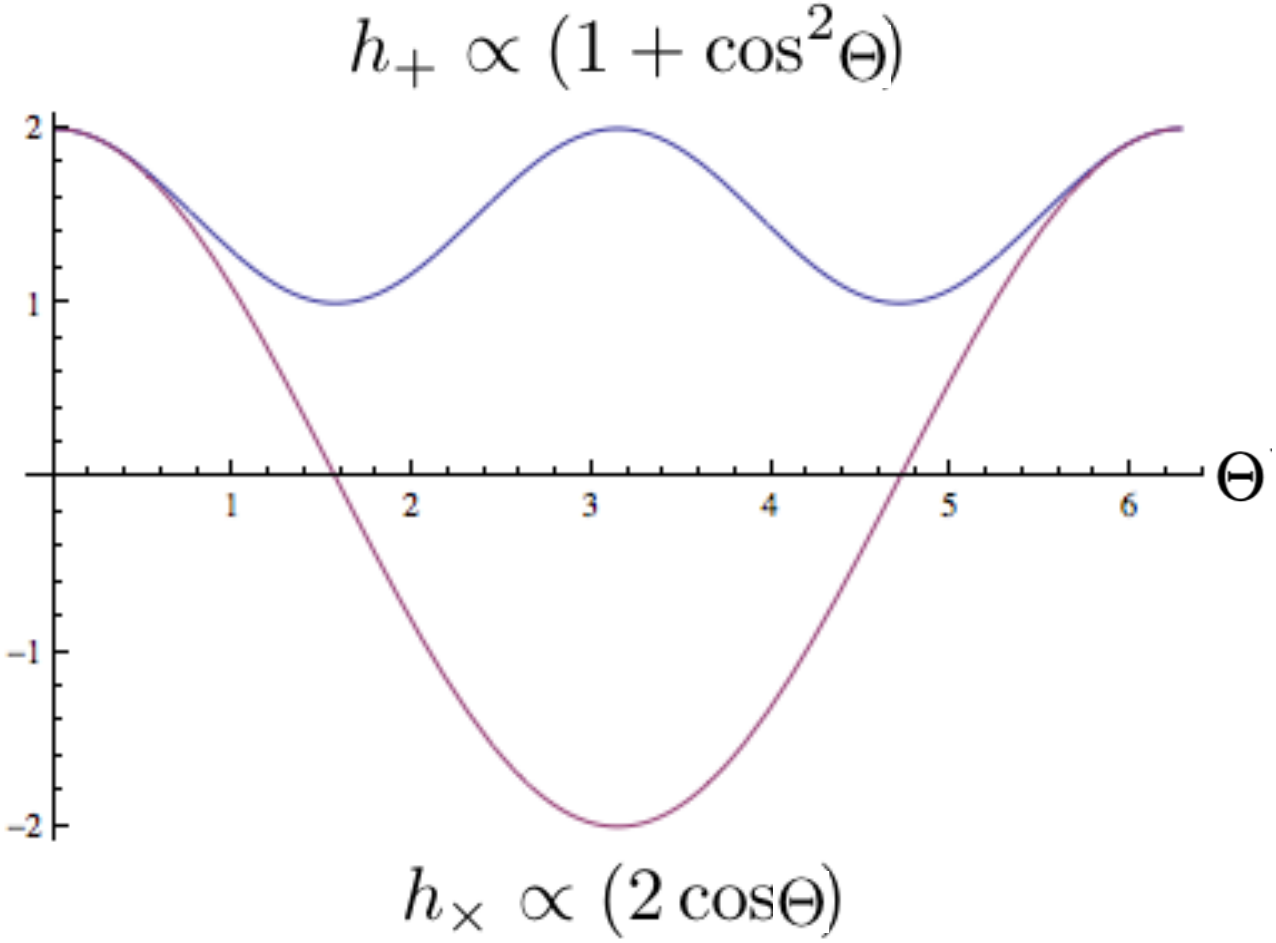

Non spinning GW polarizations (iota=0)

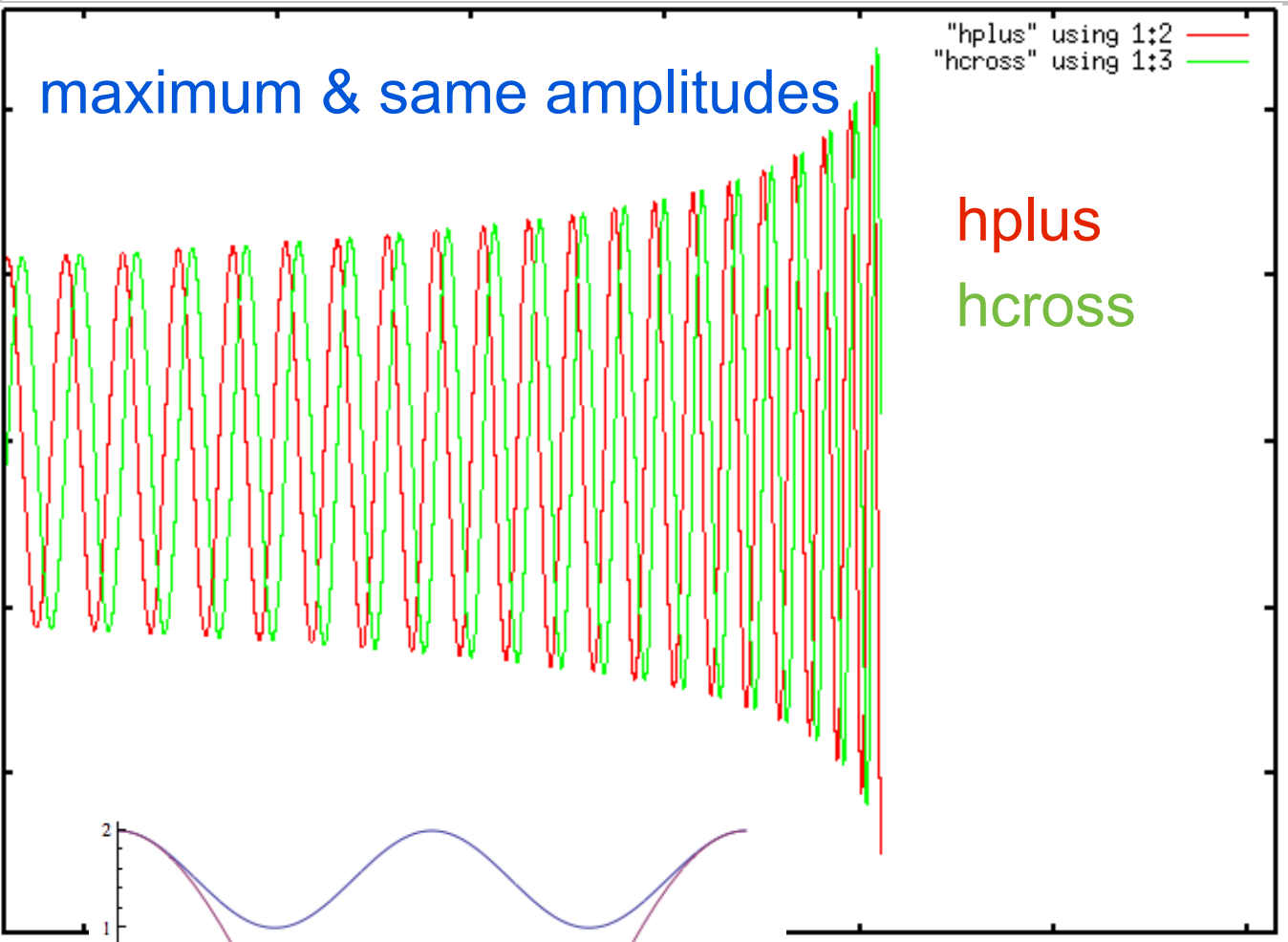

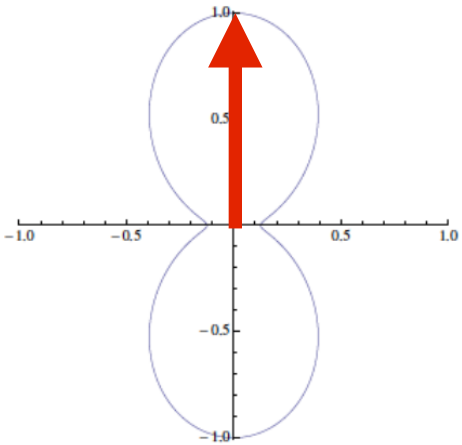

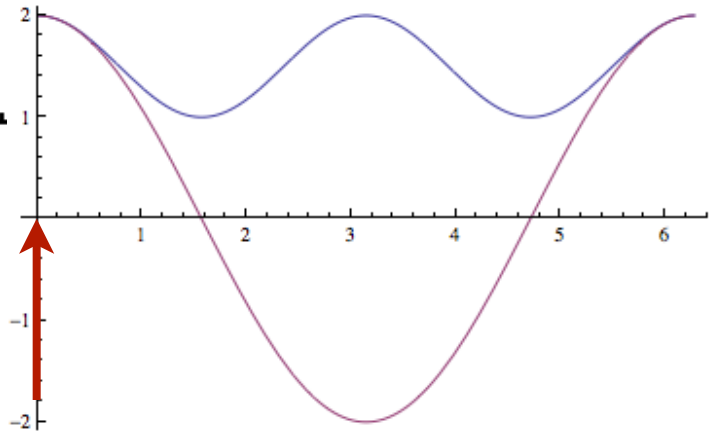

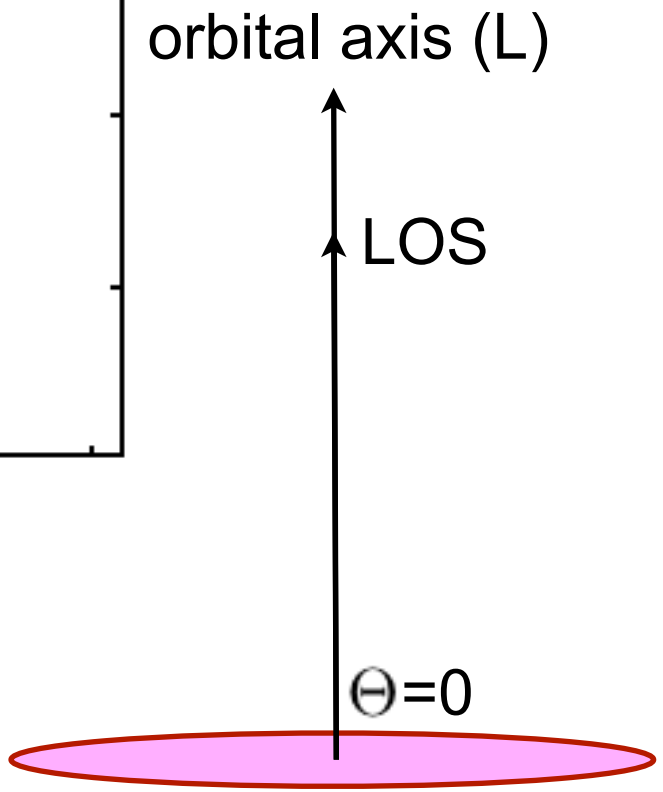

Non spinning polarizations (iota=pi/3)

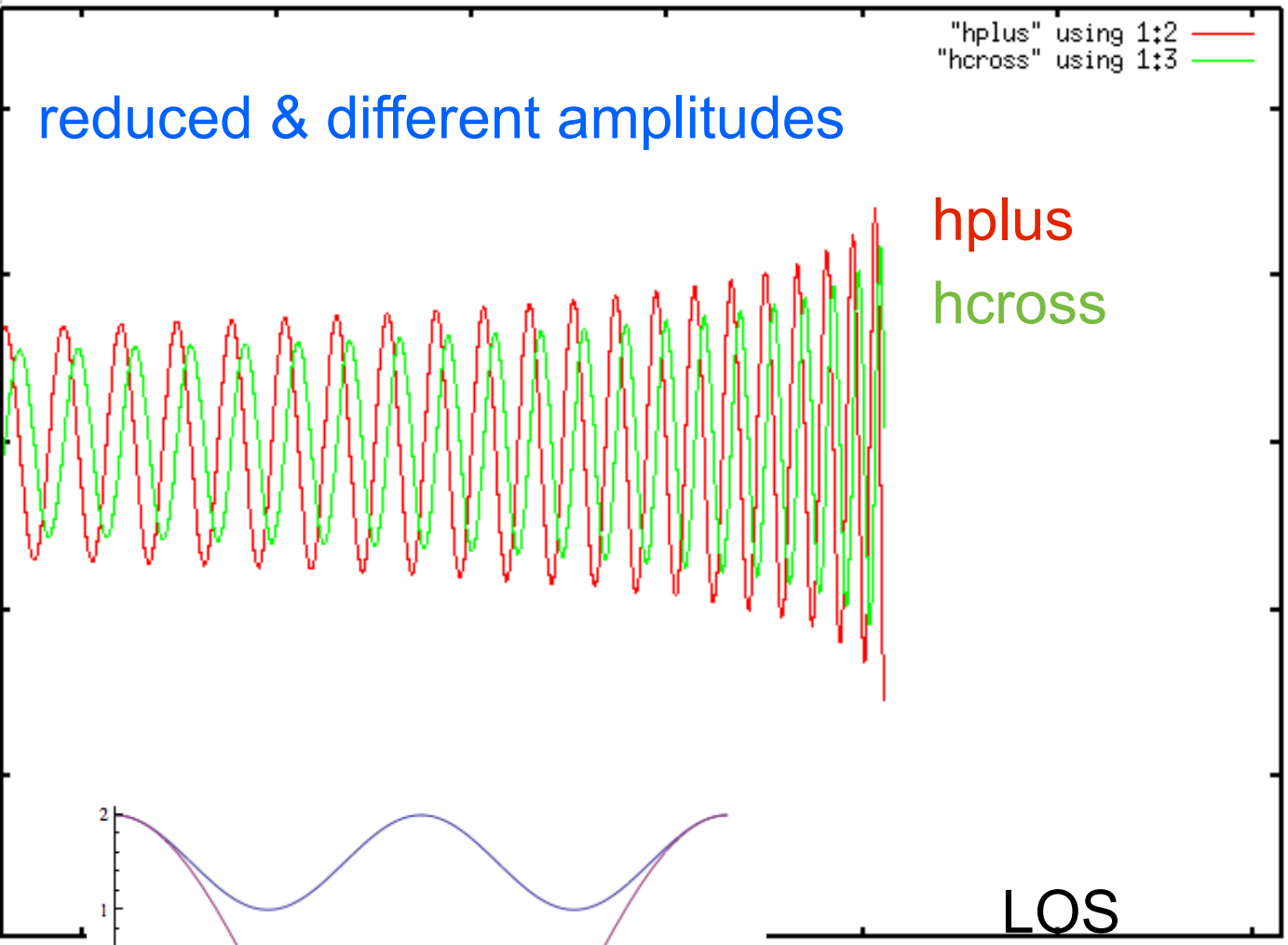

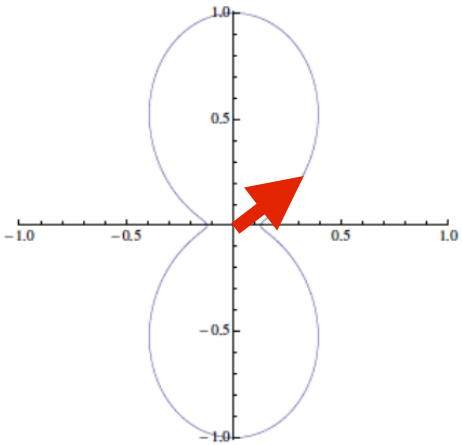

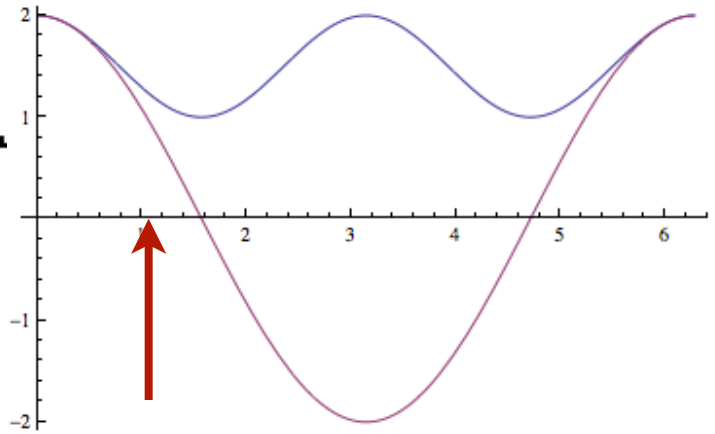

orbital axis (L)

LOS

Θ=pi/3

Non spinning polarizations (iota=pi/2)

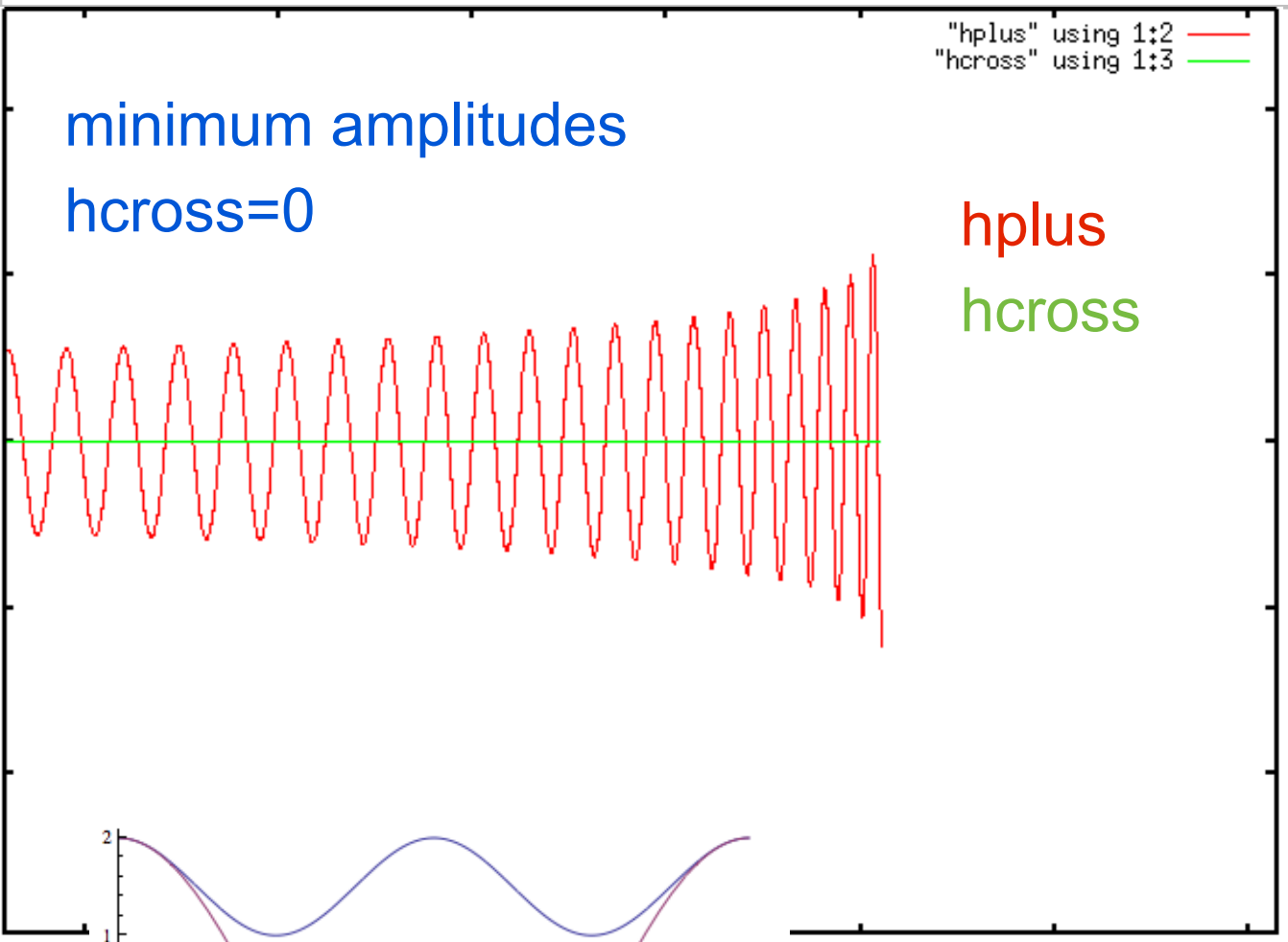

minimum amplitudes

hcross=0

hplus

hcross

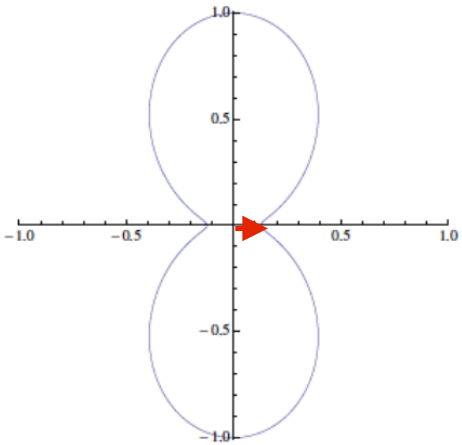

orbital axis (L)

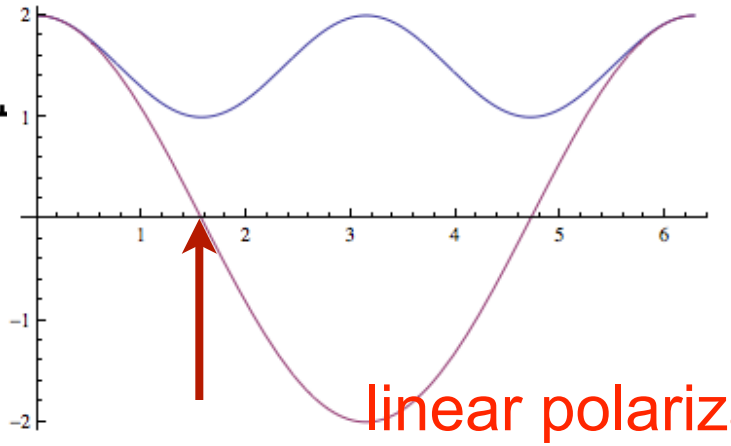

linear polarization

Θ=pi/2

LOS

distance-inclination degeneracy

$$h_+ = -\frac{2G\mu}{c^2 R} x(1+\cos^2\Theta)\cos 2\psi$$

$$h_\times = -\frac{2G\mu}{c^2 R} x(2\cos\Theta)\sin 2\psi$$

Distance

Inclination

GW170817

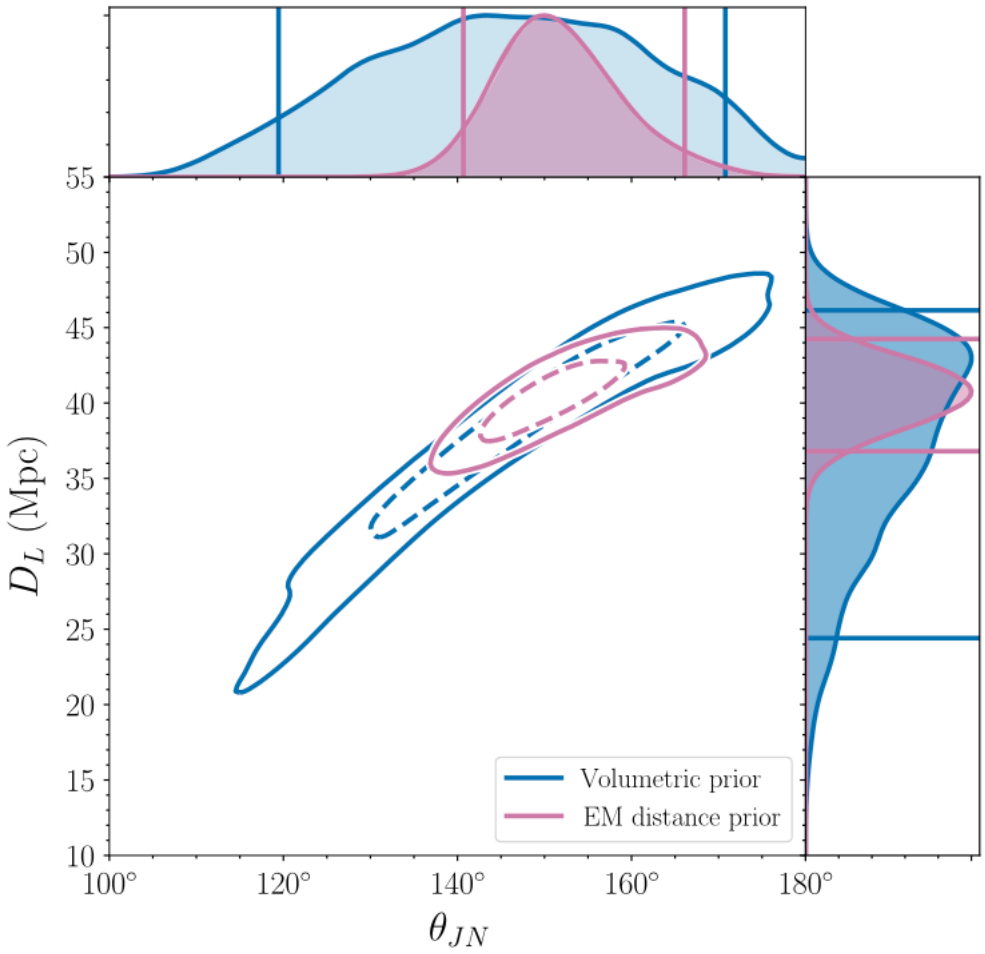

GW polarization: non spinning

$$h_+ = -\frac{2G\mu}{c^2 R} x(1+\cos^2\Theta)\cos 2\psi$$

$$h_\times = -\frac{2G\mu}{c^2 R} x(2\cos\Theta)\sin 2\psi$$

Phase evolution from post Newtonian (PN)

Post Newtonian Energy & Flux

$$E = -\frac{\mu c^2 x}{2}\left\{1 + \left(-\frac{3}{4} - \frac{1}{12}\nu\right)x + \left(-\frac{27}{8} + \frac{19}{8}\nu - \frac{1}{24}\nu^2\right)x^2 + \left(-\frac{675}{64} + \left[\frac{34445}{576} - \frac{205}{96}\pi^2\right]\nu - \frac{155}{96}\nu^2 - \frac{35}{5184}\nu^3\right)x^3\right\} + \mathcal{O}\left(\frac{1}{c^8}\right).$$

Newtonian binding energy of a binary

$$\mathcal{L} = \frac{32c^5}{5G}\nu^2 x^5\left\{1 + \left(-\frac{1247}{336} - \frac{35}{12}\nu\right)x + 4\pi x^{3/2} + \left(-\frac{44711}{9072} + \frac{9271}{504}\nu + \frac{65}{18}\nu^2\right)x^2 + \left(-\frac{8191}{672} - \frac{583}{24}\nu\right)\pi x^{5/2} + \left[\frac{6643739519}{69854400} + \frac{16}{3}\pi^2 - \frac{1712}{105}C - \frac{856}{105}\ln(16x) + \left(-\frac{134543}{7776} + \frac{41}{48}\pi^2\right)\nu - \frac{94403}{3024}\nu^2 - \frac{775}{324}\nu^3\right]x^3 + \left(-\frac{16285}{504} + \frac{214745}{1728}\nu + \frac{193385}{3024}\nu^2\right)\pi x^{7/2} + \mathcal{O}\left(\frac{1}{c^8}\right)\right\}.$$

$$x \equiv \left(\frac{G\,m\,\omega}{c^3}\right)^{2/3} \qquad m = m_1 + m_2 \qquad \mu = m_1 m_2/m \qquad \nu \equiv \frac{\mu}{m} \equiv \frac{m_1 m_2}{(m_1+m_2)^2}.$$

Phase evolution

Energy balance equation : orbital binding energy loss = GW emission energy

$$\frac{dE}{dt} = -L$$

$$\frac{dE}{dt} = \frac{dE}{dx}\frac{dx}{dt} \qquad \frac{dx}{dt} = -\frac{L}{(dE/dx)}$$

expand with x , $x \equiv \left(\frac{G\,m\,\omega}{c^3}\right)^{2/3}$

$$\frac{\dot{\omega}}{\omega^2} = \frac{96}{5}\eta(M\omega)^{5/3}\left(1 - \frac{743+924\eta}{336}(M\omega)^{2/3} + \left(\frac{34\,103}{18\,144} + \frac{13\,661}{2016}\eta + \frac{59}{18}\eta^2\right)(M\omega)^{4/3} - \frac{1}{672}(4159+14\,532\eta)\pi(M\omega)^{5/3}\eta\right.$$

$$+\left[\left(\frac{16\,447\,322\,263}{139\,708\,800} - \frac{1712}{105}\gamma_E + \frac{16}{3}\pi^2\right) + \left(-\frac{273\,811\,877}{1\,088\,640} + \frac{451}{48}\pi^2 - \frac{88}{3}\hat{\theta}\right)\eta + \frac{541}{896}\eta^2 - \frac{5605}{2592}\eta^3\right.$$

$$\left.\left. - \frac{856}{105}\log[16(M\omega)^{2/3}]\right](M\omega)^2 + \left(-\frac{4\,415}{4\,032} + \frac{661\,775}{12\,096}\eta + \frac{149\,789}{3\,024}\eta^2\right)\pi(M\omega)^{7/3}\right),$$

$$w(t) = \int_0^t \dot{w}(w)dt, \qquad \psi(t) = \int_0^t w(t)dt$$ ---> Numerical integration

TaylorT4, T1,2,3,.. : time domain models

TaylorF2

$$h(f) = \frac{M_c^{5/6}}{\pi^{2/3} D_{\rm eff}} \sqrt{\frac{5}{24}} f^{-7/6} e^{i\Psi(f)},$$

stationary phase approx.

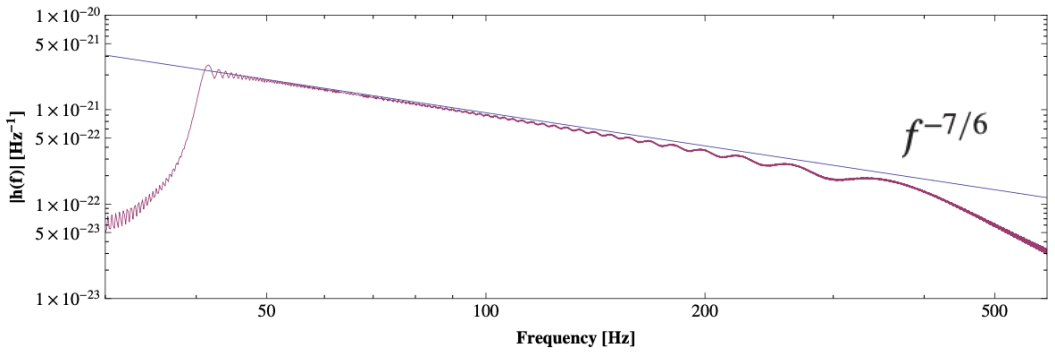

Figure 3.2: **Fourier domain TaylorT4 and SPA waveforms from a non-spinning binary.** We assume the same binary model as in figure 3.1. TaylorT4 (red) and SPA (blue) waveforms coincide at 40 Hz.

$$\begin{aligned}
\Phi_{\rm SPA}(f) &= 2\pi f t_c - \Phi_c - \frac{\pi}{4} + \frac{3}{128\nu v^5}\left\{1 + \frac{20}{9}\left(\frac{743}{336} + \frac{11}{4}\nu\right)v^2 - 16\pi v^3\right. \\
&+ 10\left(\frac{3058673}{1016064} + \frac{5429}{1008}\nu + \frac{617}{144}\nu^2\right)v^4 \qquad (3.20) \\
&+ \left(\frac{38645}{756} - \frac{65}{9}\nu\right)\left[1 + 3\log\left(\frac{v}{v_{\rm iso}}\right)\right]\pi v^5\left[\left(\frac{11583231236531}{4694215680}\right.\right. \\
&- \left.\frac{640}{3}\pi^2 - \frac{6848}{21}\gamma_E - \frac{6848}{21}\log(4v)\right) + \left(\frac{2255}{12}\pi^2 - \frac{15737765635}{3048192}\right)\nu \\
&+ \left.\left.\frac{76055}{1728}\nu^2 - \frac{127825}{1296}\nu^3\right]v^6 + \left(\frac{77096675}{254016} + \frac{378515}{1512}\nu - \frac{74045}{756}\nu^2\right)\pi v^7\right\}
\end{aligned}$$

$$v \equiv [\pi f(m_1 + m_2)]^{1/3}$$

Precession of a spinning binary

Spin-Orbit coupling, Spin-Spin coupling

$$\dot{\mathbf{S}}_1 = \frac{(M\omega)^2}{2M}\left\{\eta\,(M\omega)^{-1/3}\left(4+3\frac{m_2}{m_1}\right)\hat{\mathbf{L}}_N + \frac{1}{M^2}\left[\mathbf{S}_2 - 3(\mathbf{S}_2\cdot\hat{\mathbf{L}}_N)\hat{\mathbf{L}}_N\right]\right\}\times\mathbf{S}_1$$

$$\dot{\mathbf{S}}_2 = \frac{(M\omega)^2}{2M}\left\{\eta\,(M\omega)^{-1/3}\left(4+3\frac{m_1}{m_2}\right)\hat{\mathbf{L}}_N + \frac{1}{M^2}\left[\mathbf{S}_1 - 3(\mathbf{S}_1\cdot\hat{\mathbf{L}}_N)\hat{\mathbf{L}}_N\right]\right\}\times\mathbf{S}_2$$

$$\dot{\hat{\mathbf{L}}}_N = -\frac{(M\omega)^{1/3}}{\eta M^2}\dot{\mathbf{S}} = \frac{\omega^2}{2M}\left\{\left[\left(4+3\frac{m_2}{m_1}\right)\mathbf{S}_1 + \left(4+3\frac{m_1}{m_2}\right)\mathbf{S}_2\right]\times\hat{\mathbf{L}}_N - \frac{3\,\omega^{1/3}}{\eta\,M^{5/3}}\left[(\mathbf{S}_2\cdot\hat{\mathbf{L}}_N)\,\mathbf{S}_1 + (\mathbf{S}_1\cdot\hat{\mathbf{L}}_N)\,\mathbf{S}_2\right]\times\hat{\mathbf{L}}_N\right\}$$

precession

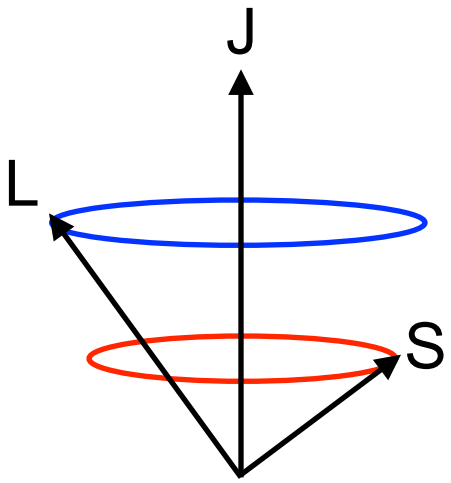

|J| ↓

|L| ↓

|s| =const.

Precession of a spinning binary

Spin-Orbit coupling, Spin-Spin coupling

$$\dot{\mathbf{S}}_1 = \frac{(M\omega)^2}{2M}\left\{\eta\,(M\omega)^{-1/3}\left(4+3\frac{m_2}{m_1}\right)\hat{\mathbf{L}}_N + \frac{1}{M^2}\left[\mathbf{S}_2 - 3(\mathbf{S}_2\cdot\hat{\mathbf{L}}_N)\hat{\mathbf{L}}_N\right]\right\}\times\mathbf{S}_1$$

$$\dot{\mathbf{S}}_2 = \frac{(M\omega)^2}{2M}\left\{\eta\,(M\omega)^{-1/3}\left(4+3\frac{m_1}{m_2}\right)\hat{\mathbf{L}}_N + \frac{1}{M^2}\left[\mathbf{S}_1 - 3(\mathbf{S}_1\cdot\hat{\mathbf{L}}_N)\hat{\mathbf{L}}_N\right]\right\}\times\mathbf{S}_2$$

$$\dot{\hat{\mathbf{L}}}_N = -\frac{(M\omega)^{1/3}}{\eta M^2}\dot{\mathbf{S}} = \frac{\omega^2}{2M}\left\{\left[\left(4+3\frac{m_2}{m_1}\right)\mathbf{S}_1 + \left(4+3\frac{m_1}{m_2}\right)\mathbf{S}_2\right]\times\hat{\mathbf{L}}_N - \frac{3\,\omega^{1/3}}{\eta\,M^{5/3}}\left[(\mathbf{S}_2\cdot\hat{\mathbf{L}}_N)\,\mathbf{S}_1 + (\mathbf{S}_1\cdot\hat{\mathbf{L}}_N)\,\mathbf{S}_2\right]\times\hat{\mathbf{L}}_N\right\}$$

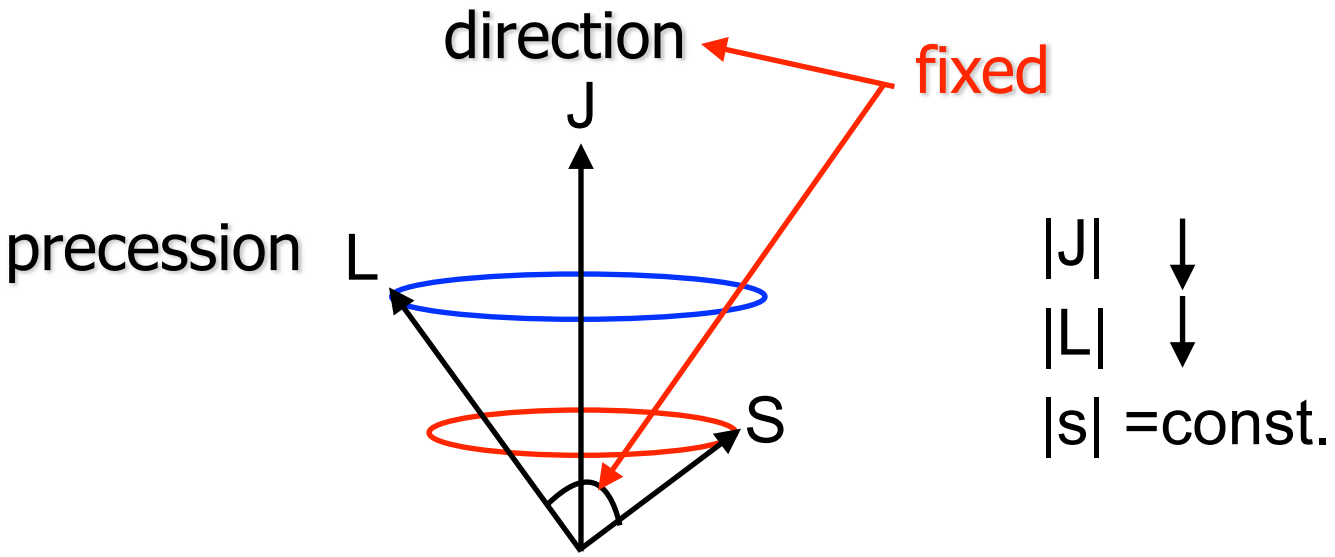

Precession of a spinning binary

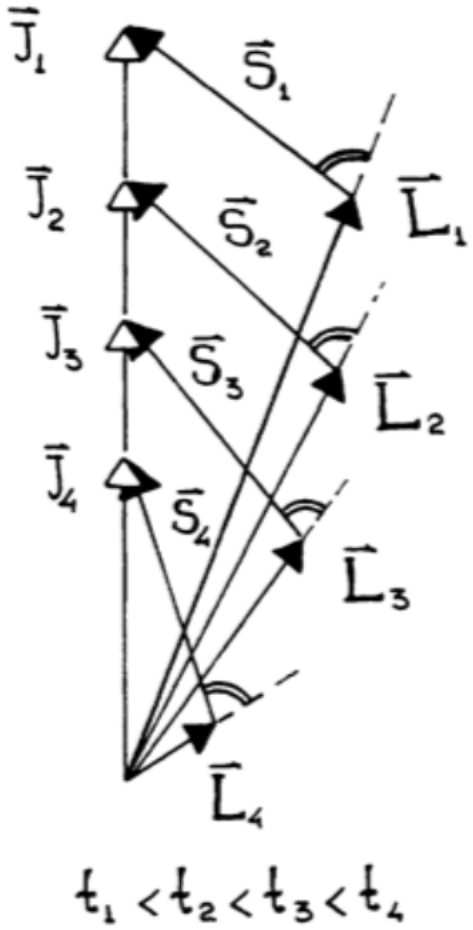

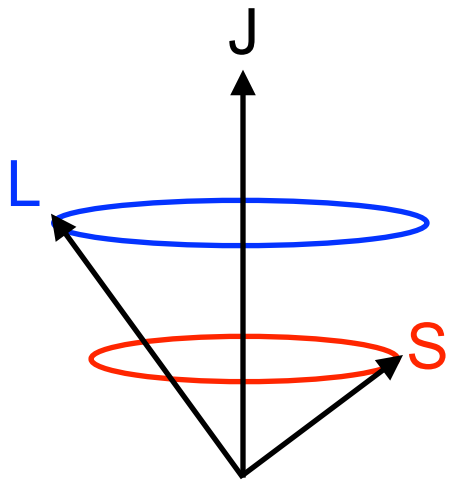

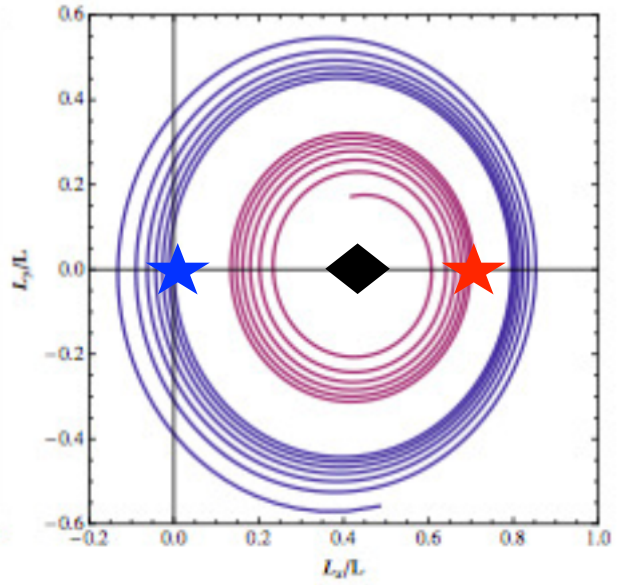

GW Polarization of spinning binary

$$h_+ = -\frac{2G\mu}{c^2 R} x [C_+ \cos 2\psi + S_+ \sin 2\psi]$$

$$h_\times = -\frac{2G\mu}{c^2 R} x [C_\times \cos 2\psi + S_\times \sin 2\psi]$$

non spinning

$$h_+ = -\frac{2G\mu}{c^2 R} x (1 + \cos^2 \Theta) \cos 2\psi$$

$$h_\times = -\frac{2G\mu}{c^2 R} x (2 \cos \Theta) \sin 2\psi$$

$$C_+ = \tfrac{1}{2}\cos^2\Theta\,(\sin^2\alpha - \cos^2 i \cos^2\alpha) + \tfrac{1}{2}(\cos^2 i \sin^2\alpha - \cos^2\alpha) - \tfrac{1}{2}\sin^2\Theta \sin^2 i - \tfrac{1}{4}\sin 2\Theta \sin 2i \cos\alpha,$$

$$S_+ = \tfrac{1}{2}\,(1 + \cos^2\Theta)\cos i \sin 2\alpha + \tfrac{1}{2}\sin 2\Theta \sin i \sin\alpha,$$

$$C_\times = -\tfrac{1}{2}\cos\Theta \sin 2\alpha\,(1 + \cos^2 i) - \tfrac{1}{2}\sin\Theta \sin 2i \sin\alpha,$$

$$S_\times = -\cos\Theta \cos i \cos 2\alpha - \sin\Theta \sin i \cos\alpha,$$

ι, α, Θ : vary in time

--> precessional motion

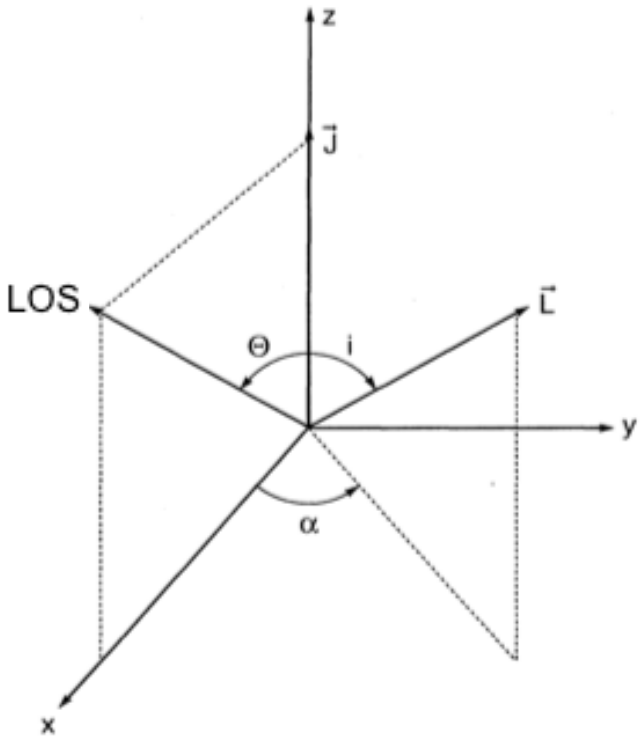

Precession equations

Spin-Orbit coupling, Spin-Spin coupling

$$\dot{\mathbf{S}}_1 = \frac{(M\omega)^2}{2M}\left\{\eta\,(M\omega)^{-1/3}\left(4+3\frac{m_2}{m_1}\right)\hat{\mathbf{L}}_N+\frac{1}{M^2}\left[\mathbf{S}_2-3(\mathbf{S}_2\cdot\hat{\mathbf{L}}_N)\hat{\mathbf{L}}_N\right]\right\}\times\mathbf{S}_1$$

$$\dot{\mathbf{S}}_2 = \frac{(M\omega)^2}{2M}\left\{\eta\,(M\omega)^{-1/3}\left(4+3\frac{m_1}{m_2}\right)\hat{\mathbf{L}}_N+\frac{1}{M^2}\left[\mathbf{S}_1-3(\mathbf{S}_1\cdot\hat{\mathbf{L}}_N)\hat{\mathbf{L}}_N\right]\right\}\times\mathbf{S}_2$$

$$\dot{\hat{\mathbf{L}}}_N = -\frac{(M\omega)^{1/3}}{\eta M^2}\dot{\mathbf{S}} = \frac{\omega^2}{2M}\left\{\left[\left(4+3\frac{m_2}{m_1}\right)\mathbf{S}_1+\left(4+3\frac{m_1}{m_2}\right)\mathbf{S}_2\right]\times\hat{\mathbf{L}}_N - \frac{3\,\omega^{1/3}}{\eta\,M^{5/3}}\left[(\mathbf{S}_2\cdot\hat{\mathbf{L}}_N)\,\mathbf{S}_1+(\mathbf{S}_1\cdot\hat{\mathbf{L}}_N)\,\mathbf{S}_2\right]\times\hat{\mathbf{L}}_N\right\}$$

phase equation has additional spin terms !!

$$\frac{\dot{\omega}}{\omega^2} = \frac{96}{5}\eta(M\omega)^{5/3}\left(1-\frac{743+924\eta}{336}(M\omega)^{2/3}-\left\{\frac{1}{12}\sum_{i=1,2}\left[\chi_i(\hat{\mathbf{L}}_N\cdot\hat{\mathbf{S}}_i)\left(113\frac{m_i^2}{M^2}+75\eta\right)\right]-4\pi\right\}(M\omega)+\left(\frac{34\,103}{18\,144}+\frac{13\,661}{2016}\eta\right.\right.$$
$$\left.+\frac{59}{18}\eta^2\right)(M\omega)^{4/3}-\frac{1}{48}\eta\chi_1\chi_2[247(\hat{\mathbf{S}}_1\cdot\hat{\mathbf{S}}_2)-721(\hat{\mathbf{L}}_N\cdot\hat{\mathbf{S}}_1)(\hat{\mathbf{L}}_N\cdot\hat{\mathbf{S}}_2)](M\omega)^{4/3}-\frac{1}{672}(4159+14\,532\eta)\pi(M\omega)^{5/3}$$
$$+\left[\left(\frac{16\,447\,322\,263}{139\,708\,800}-\frac{1712}{105}\gamma_E+\frac{16}{3}\pi^2\right)+\left(-\frac{273\,811\,877}{1\,088\,640}+\frac{451}{48}\pi^2-\frac{88}{3}\hat{\theta}\right)\eta+\frac{541}{896}\eta^2-\frac{5605}{2592}\eta^3\right.$$
$$\left.\left.-\frac{856}{105}\log[16(M\omega)^{2/3}]\right](M\omega)^2+\left(-\frac{4\,415}{4\,032}+\frac{661\,775}{12\,096}\eta+\frac{149\,789}{3\,024}\eta^2\right)\pi(M\omega)^{7/3}\right), \qquad (1)$$

Waveform of spinning binary

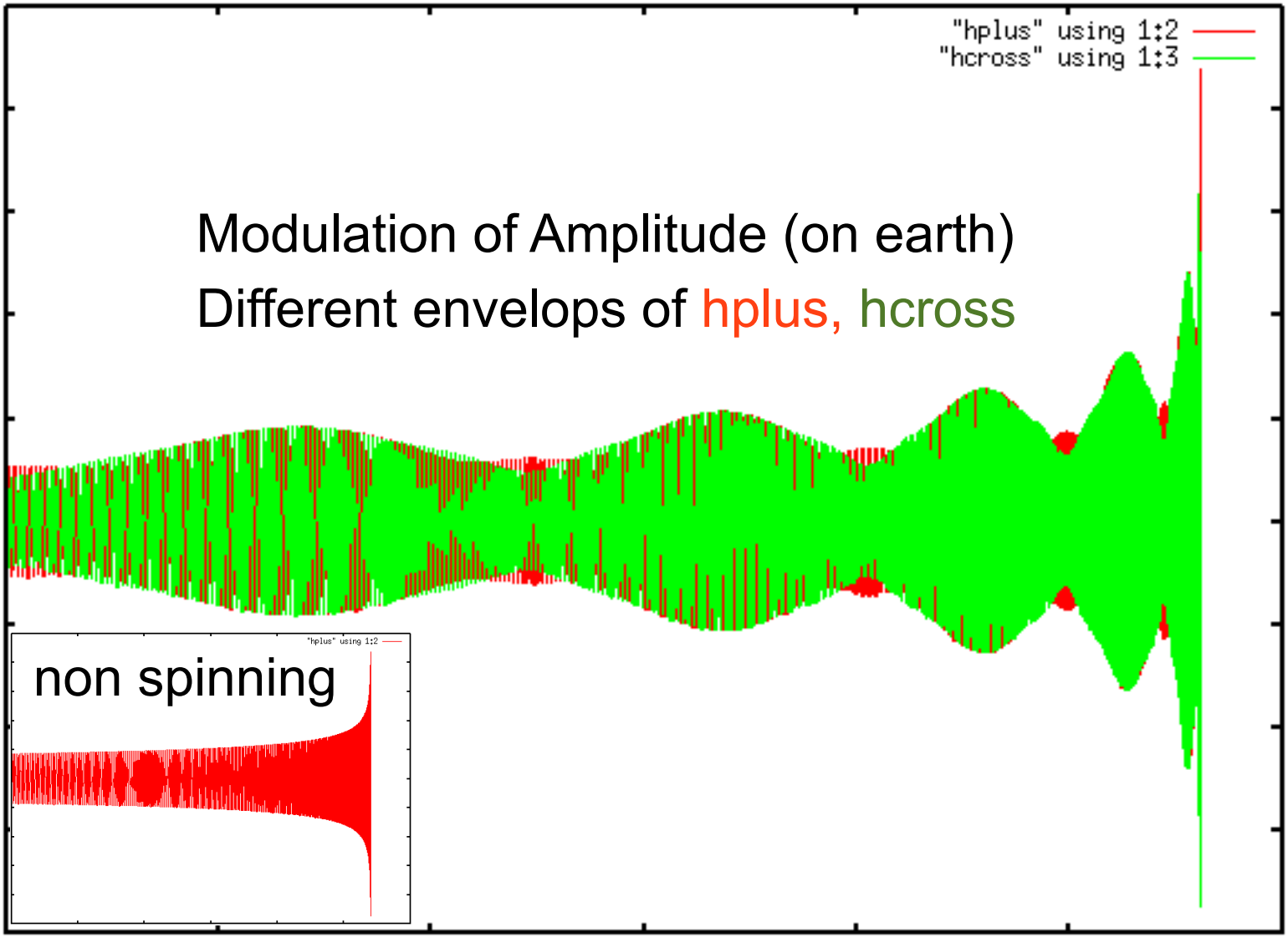

Modulation magnitude

Variation of L_N depends on S, S dot L_N, S cross L_N

---> Precession effect depends on

1) Spin magnitude
2) Angle between L_N and S

$$\dot{\hat{\mathbf{L}}}_N = -\frac{(M\omega)^{1/3}}{\eta M^2}\dot{\mathbf{S}} = \frac{\omega^2}{2M}\left\{ \left[\left(4+3\frac{m_2}{m_1}\right)\mathbf{S}_1 + \left(4+3\frac{m_1}{m_2}\right)\mathbf{S}_2\right]\times\hat{\mathbf{L}}_N \right.$$
$$\left. -\frac{3\,\omega^{1/3}}{\eta\, M^{5/3}}\left[(\mathbf{S}_2\cdot\hat{\mathbf{L}}_N)\,\mathbf{S}_1 + (\mathbf{S}_1\cdot\hat{\mathbf{L}}_N)\,\mathbf{S}_2\right]\times\hat{\mathbf{L}}_N \right\}$$

Amplitude modulation with Spin (Angle=pi/2, S2=0)

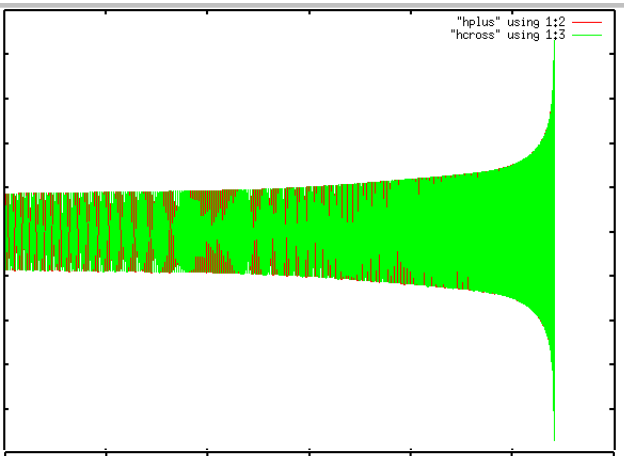

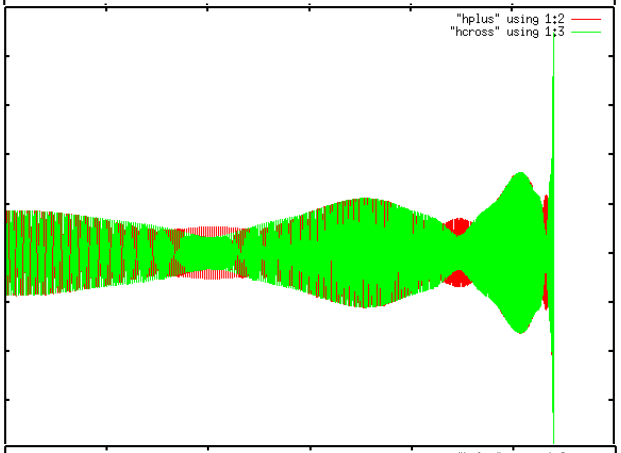

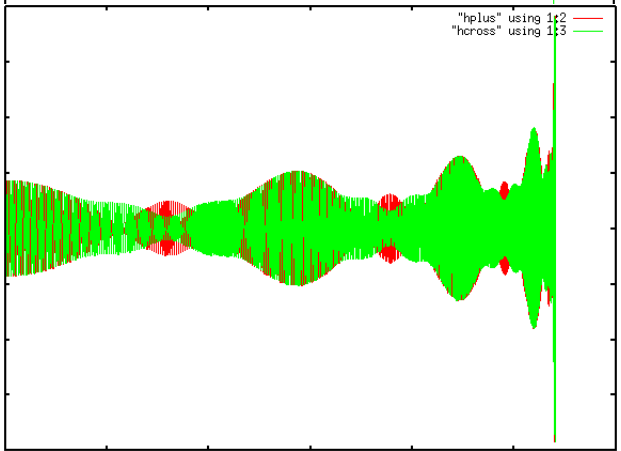

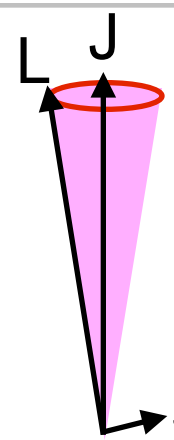

NS-NS binary

precessing cone

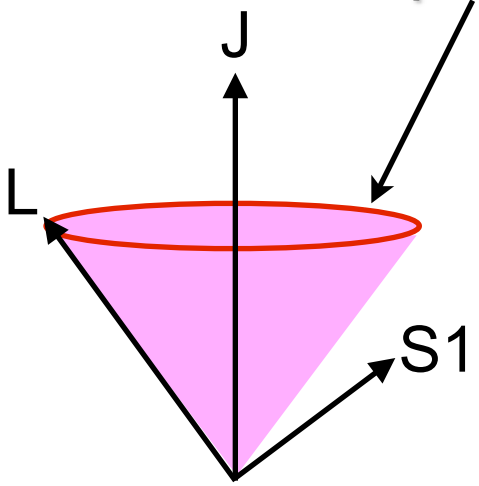

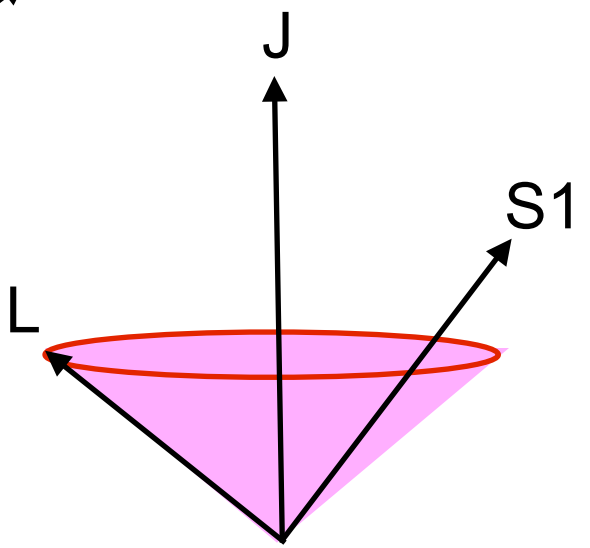

Amplitude modulation with Angle (a1=0.9, S2=0)

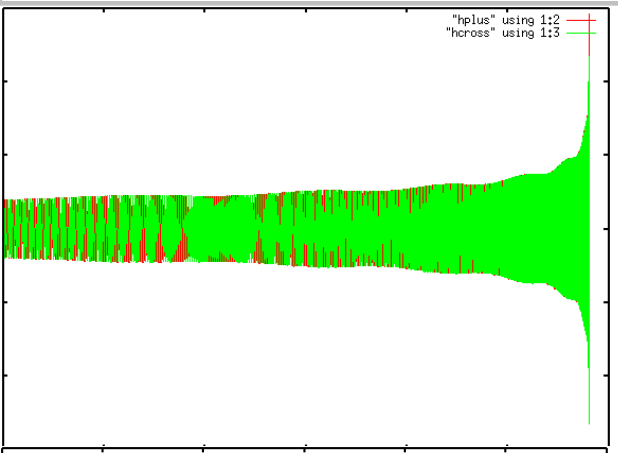

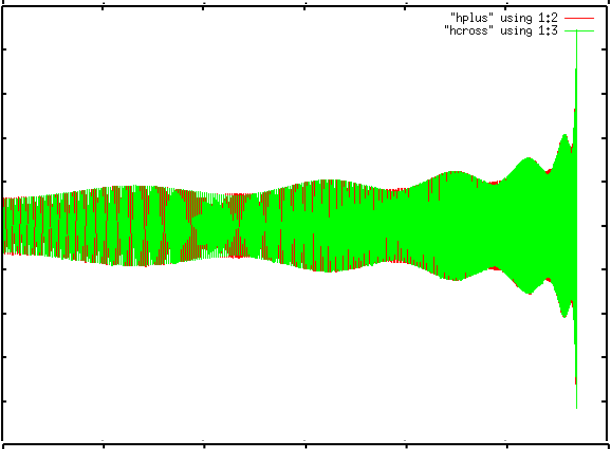

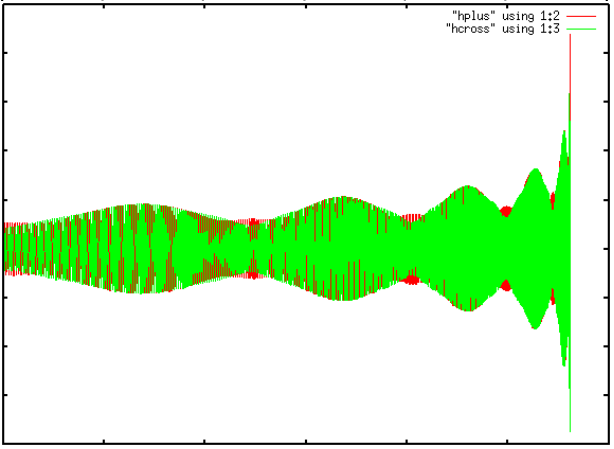

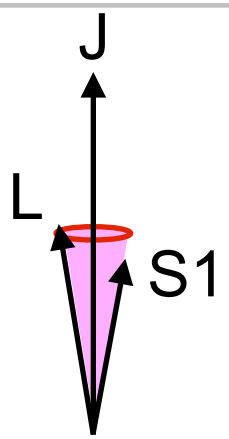

aligned-spin: no precession

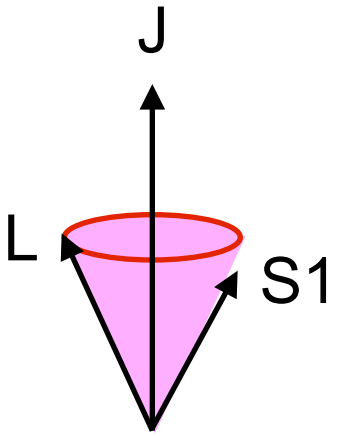

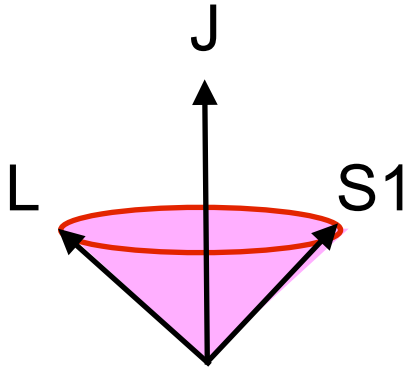

Detected wave strain (detector frame)

- The gravitational-wave signal is a combination of two polarizations:

$$h_{\text{resp}} = F_+ h_+ + F_\times h_\times$$

F_+ and F_x : detector response functions

$$F_+ = \frac{1}{2}(1+\cos^2\theta)\cos 2\phi \cos 2\psi - \cos\theta \sin 2\phi \sin 2\psi,$$

$$F_\times = \frac{1}{2}(1+\cos^2\theta)\cos 2\phi \sin 2\psi + \cos\theta \sin 2\phi \cos 2\psi.$$

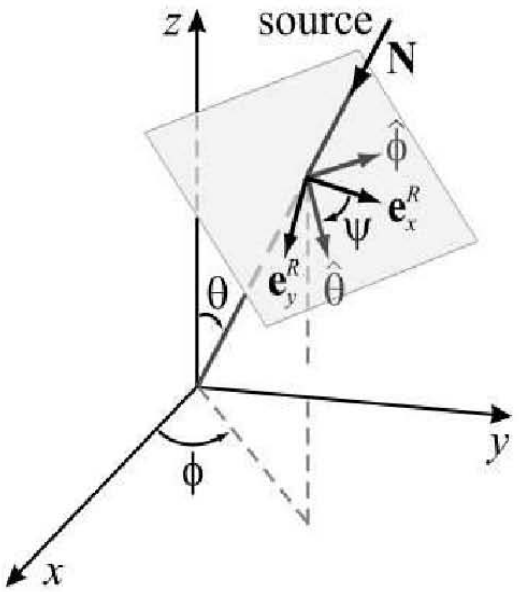

Depend on sky location (θ, ϕ) and polarization angle ψ

Detector response versus sky location

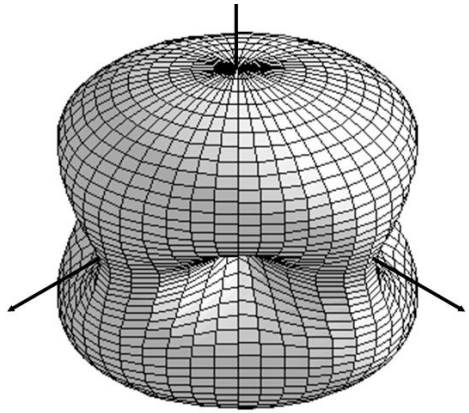

4 hidden positions
for a single detector

Waveform modeling

- **Post-Newtonian (PN) approximation**: slow motion approximation $(v/c << 1)$
- **Perturbative theory**: small mass ratio $(m/M \ll 1)$
- **Effective-One-Body approach**: combination of PN, Perturbative approach and NR

Binary parameter space

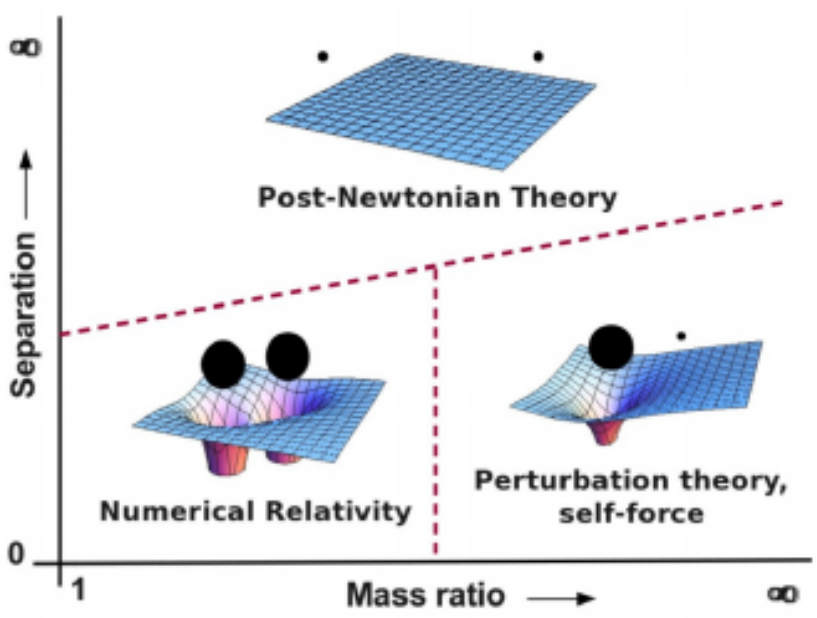

[Leor Barack]

Waveform modeling: Effective-One-Body and Phenomenological Model

EOB: mapping two body problem to a test mass moving in effective perturbed Kerr spacetime

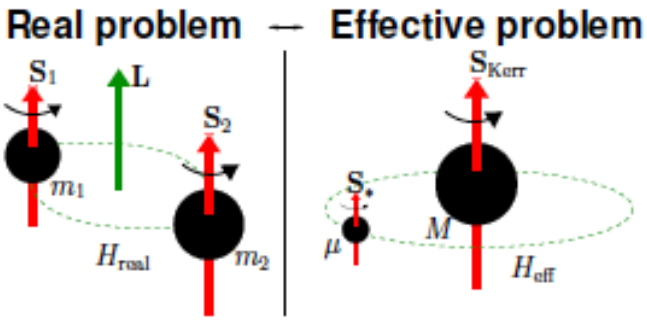

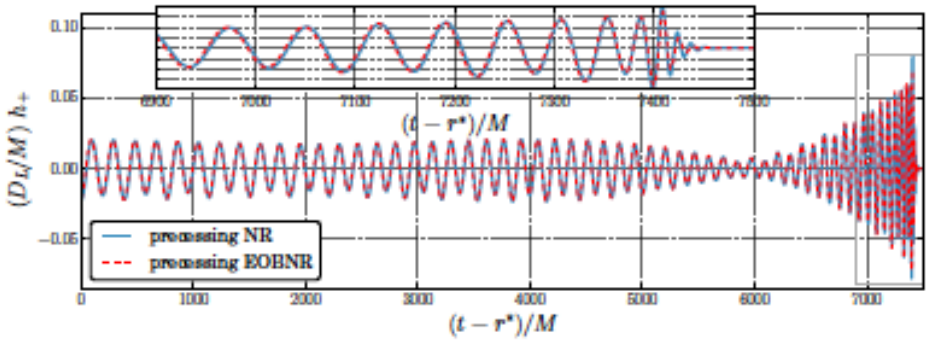

[Babak+ PRD, 2016]

IMRPhenom: phenomenological approach uses PN for inspiral and fit for the late IMR

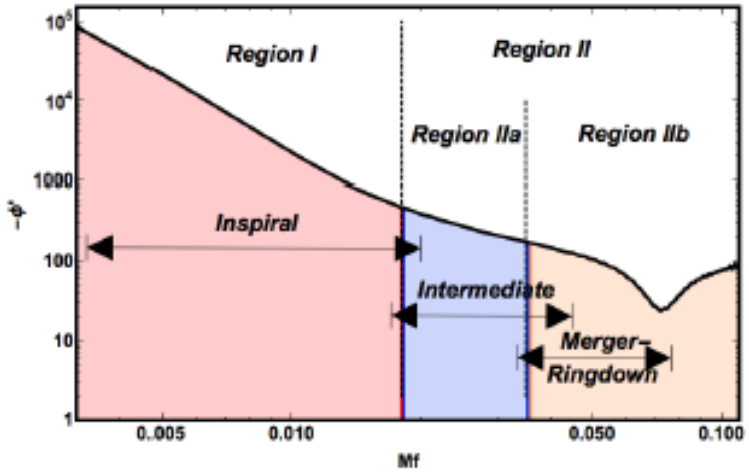

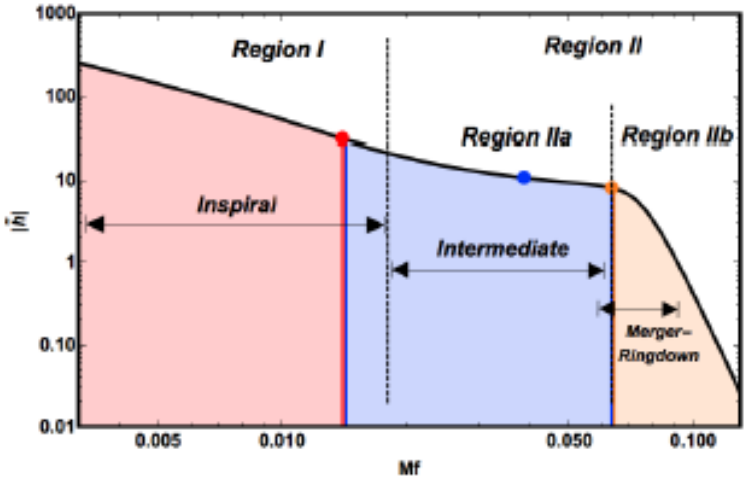

[Khan+ PRD, 2016]

Waveform modeling: Effective-One-Body and

Family	Short name	Full name	Precession	Multipoles $(\ell, \lvert m \rvert)$	Reference
EOBNR	EOBNR	SEOBNRv4_ROM	✗	(2, 2)	[57]
	EOBNR HM	SEOBNRv4HM_ROM	✗	(2, 2), (2,1), (3, 3), (4, 4), (5, 5)	[26,32]
	EOBNR P	SEOBNRv4P	✓	(2, 2), (2, 1)	[33,118,119]
	EOBNR PHM	SEOBNRv4PHM	✓	(2, 2), (2, 1), (3, 3), (4, 4), (5, 5)	[33,118,119]
Phenom	Phenom	IMRPhenomD	✗	(2, 2)	[120,121]
	Phenom HM	IMRPhenomHM	✗	(2, 2), (2, 1), (3, 3), (3, 2), (4, 4), (4, 3)	[22]
	Phenom P	IMRPhenomPv2/v3[a]	✓	(2, 2)	[23,122]
	Phenom PHM	IMRPhenomPv3HM	✓	(2, 2), (2, 1), (3, 3), (3, 2), (4, 4), (4, 3)	[24]

$H_{\rm real}$ m_2 μ $H_{\rm eff}$ 0 1000 2000 3000 4000 5000 6000 7000 $(t-r^*)/M$

IMRPhenom:

t for the late IMR

Full name (implemented in LAL) Short label (used in this work)	References Base model	 Corrections
SEOBNRv4_ROM_NRTidalv2 SEOBNR_T	[14–16]	[17, 18]
SEOBNRv4_ROM_NRTidalv2_NSBH [19] SEOBNR_NSBH	[14–16]	[17, 18, 20]
IMRPhenomPv2_NRTidalv2 IMRPhenomP_T	[21–23]	[17, 18]
IMRPhenomNSBH [24] IMRPhenom_NSBH	[25]	[18, 20]

TABLE I: Waveform models used in our analysis for NSBH systems.

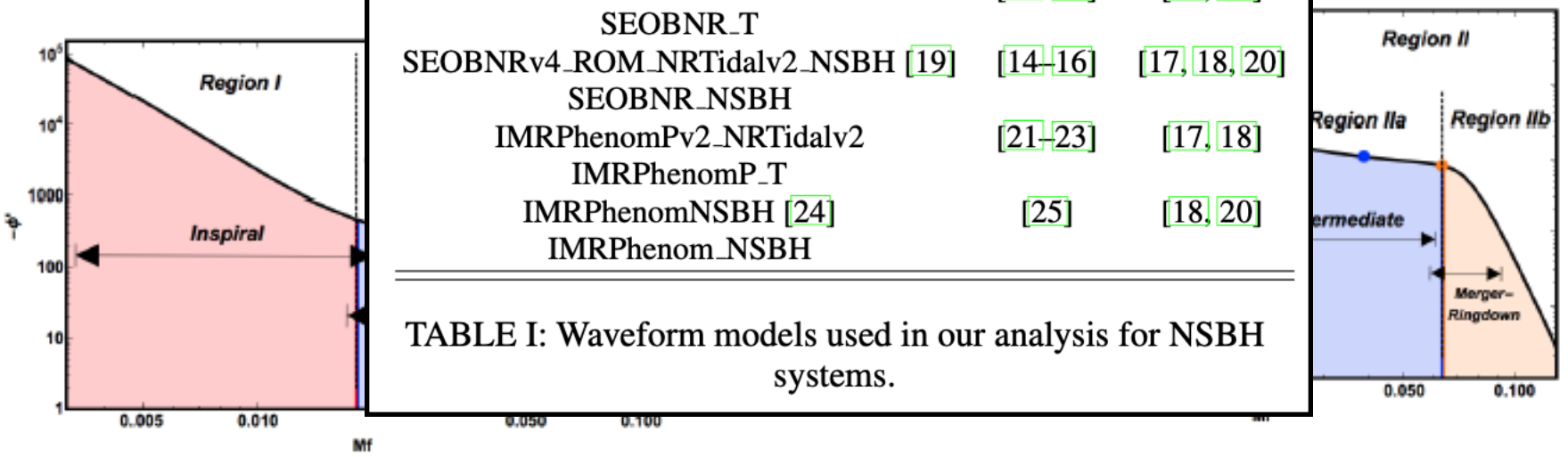

[Khan+ PRD, 2016]

Why full IMR waveforms ?

	m_1 / m_2	f_{ISCO}
NS-NS	1.4 /1.4 $M_\odot$	1600 Hz
BH-BH	17.5/17.5 $M_\odot$	128 Hz

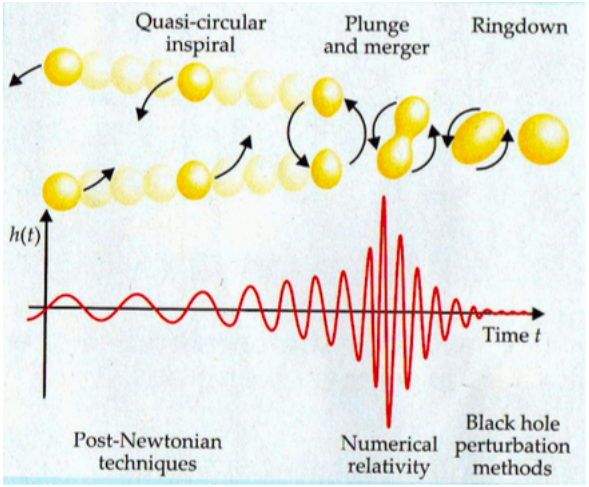

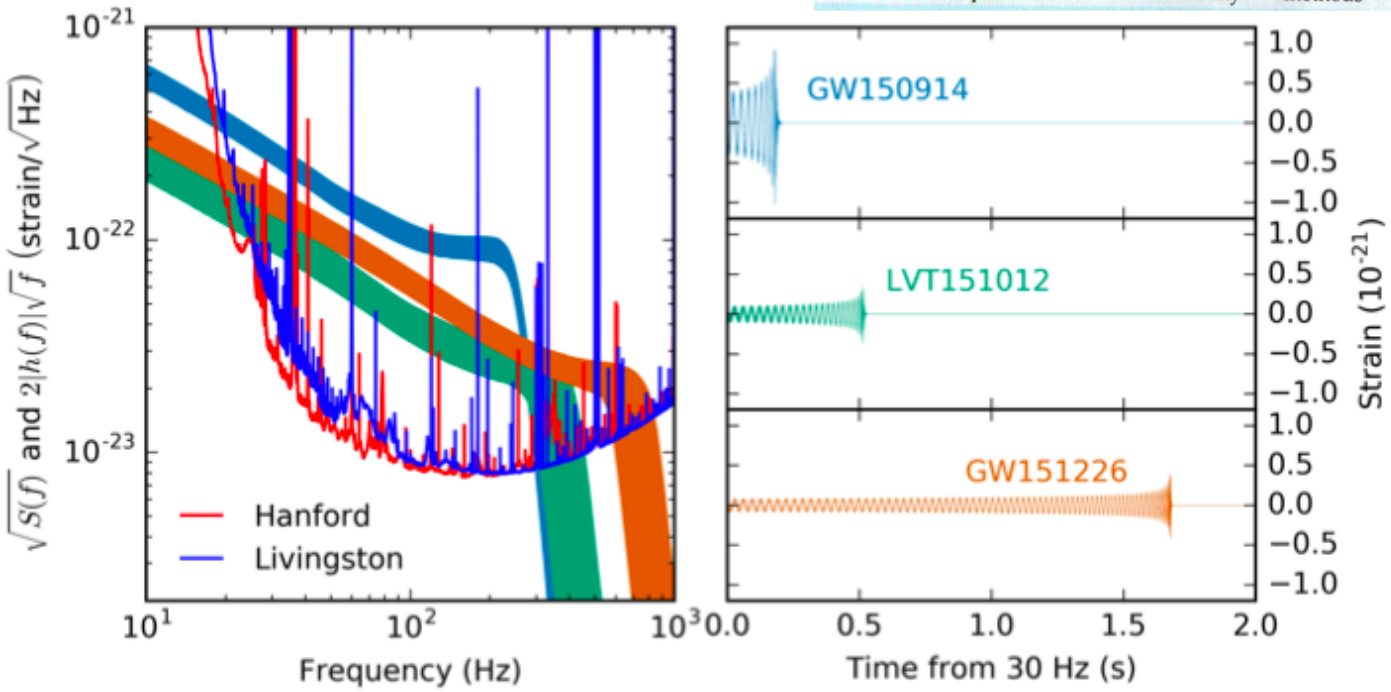

Outline

- Compact Binary Coalescence (CBC) waveforms
  - nonspinning
  - precessing (amplitude modulation)
  - PN phase evolution
  - waveform models

- CBC data analysis
  - matched filter
  - efficiency of template bank: fitting factor
  - detection & parameter estimation

- Systematic error in parameter estimation
  - examples
  - impact of eccentricity (review on recent works)

detection method: Matched filtering

- Matched filtering is the optimal filter for a signal of known shape in the stationary Gaussian noise
- 1) Known signal ? CBC GW waveform models
- 2) Stationary Gaussian noise ? real noises often give false alarms without a true signal

Matched filtering

Match $$\left\langle \tilde{h}_s \middle| \tilde{h}_t \right\rangle = 4\,\mathrm{Re}\int_{f_{low}}^{\infty} \frac{\tilde{h}_s(f)\tilde{h}_t^*(f)}{S_n(f)}\mathrm{d}f,$$

Detector output (d)

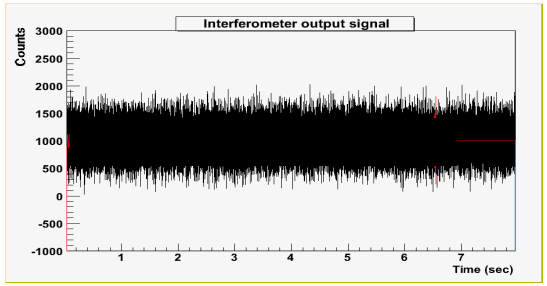

or

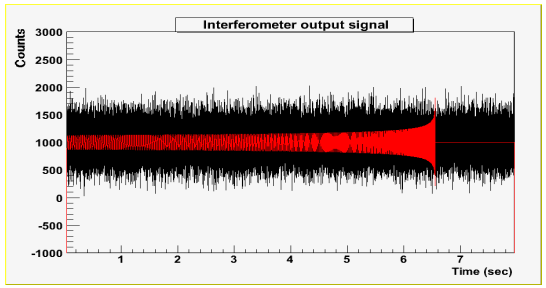

⊗

Model waveform (T)

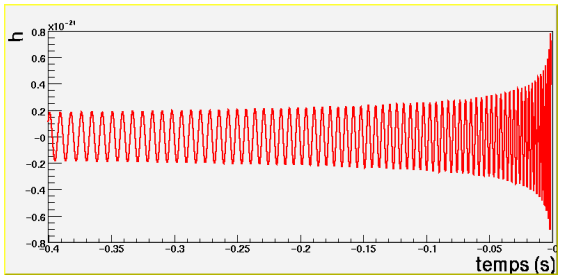

/

Detector noise sensitivity (S_n)

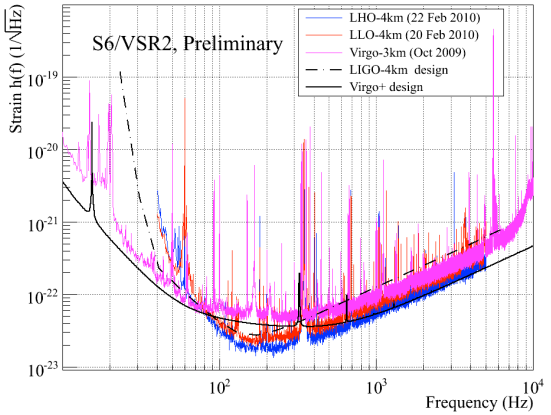

$$S(t) = 4\int_{f_{low}}^{f_{final}} \frac{\tilde{d}(f)\ \tilde{T}^*(f)}{S_n(f)}\ e^{2\pi i f t}\ df$$ ==>

Signal To Noise Ratio

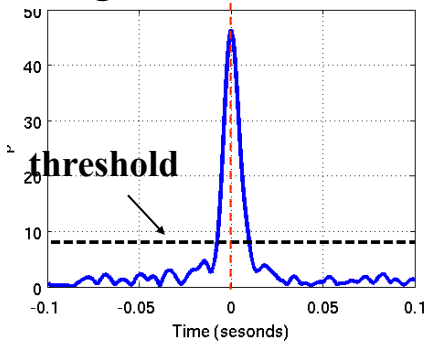

$$SNR = \frac{\langle S \rangle}{\sqrt{\langle N^2 \rangle}}$$

Matched filtering

We are searching for a signal of a specific shape buried in the noise: matched filtering.

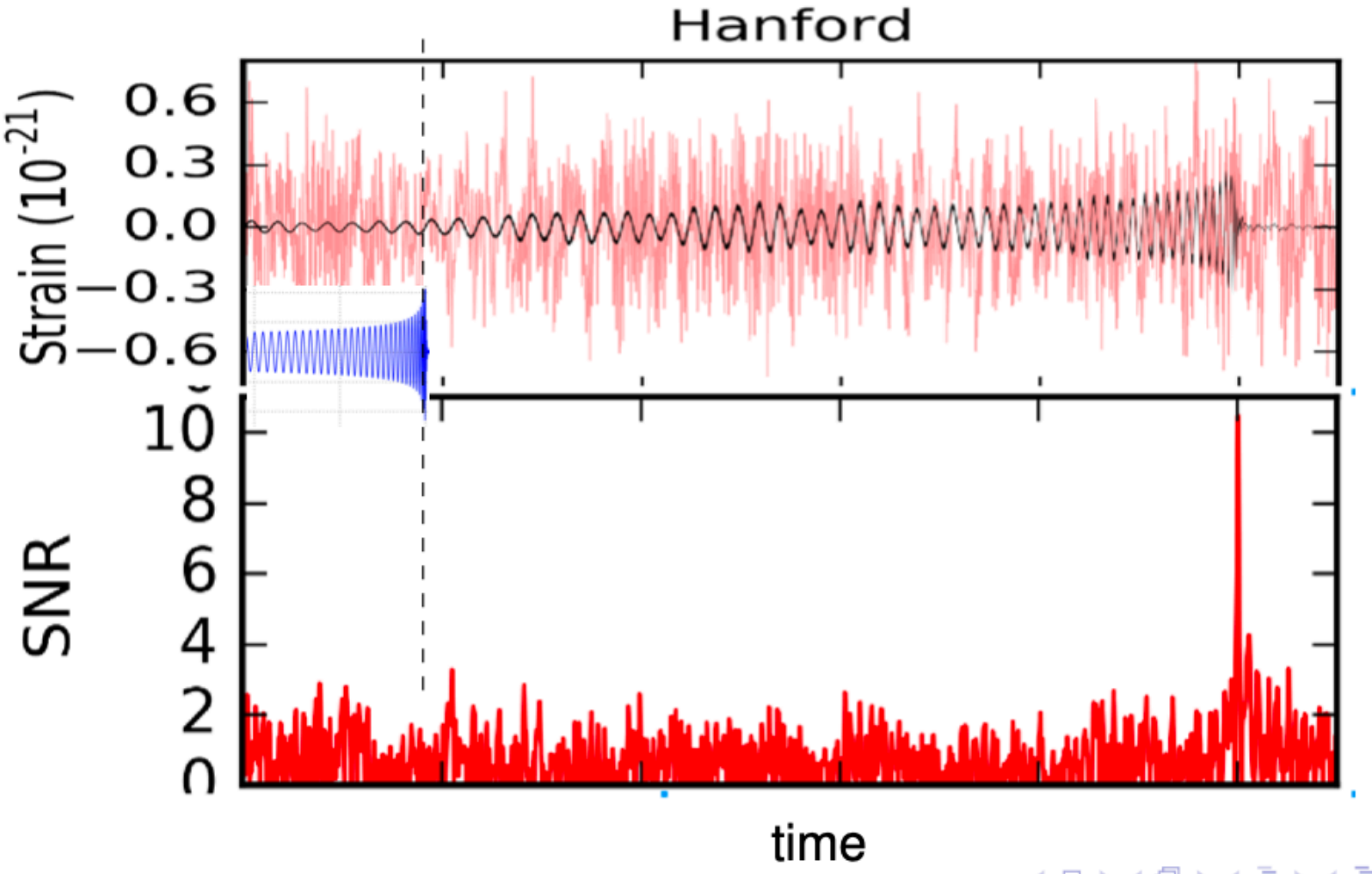

Matched filtering

We are searching for a signal of a specific shape buried in the noise: matched filtering.

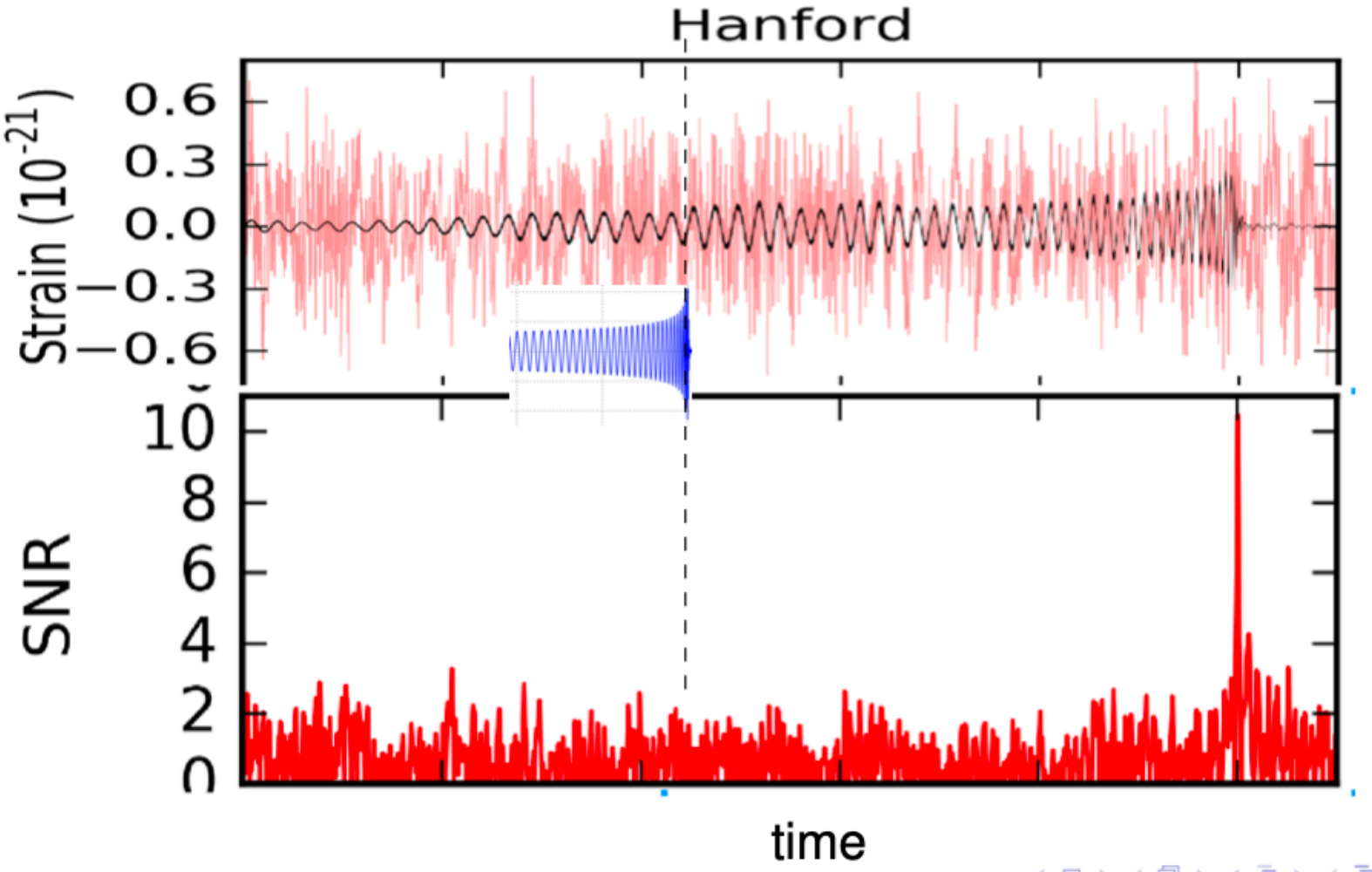

Matched filtering

We are searching for a signal of a specific shape buried in the noise: matched filtering.

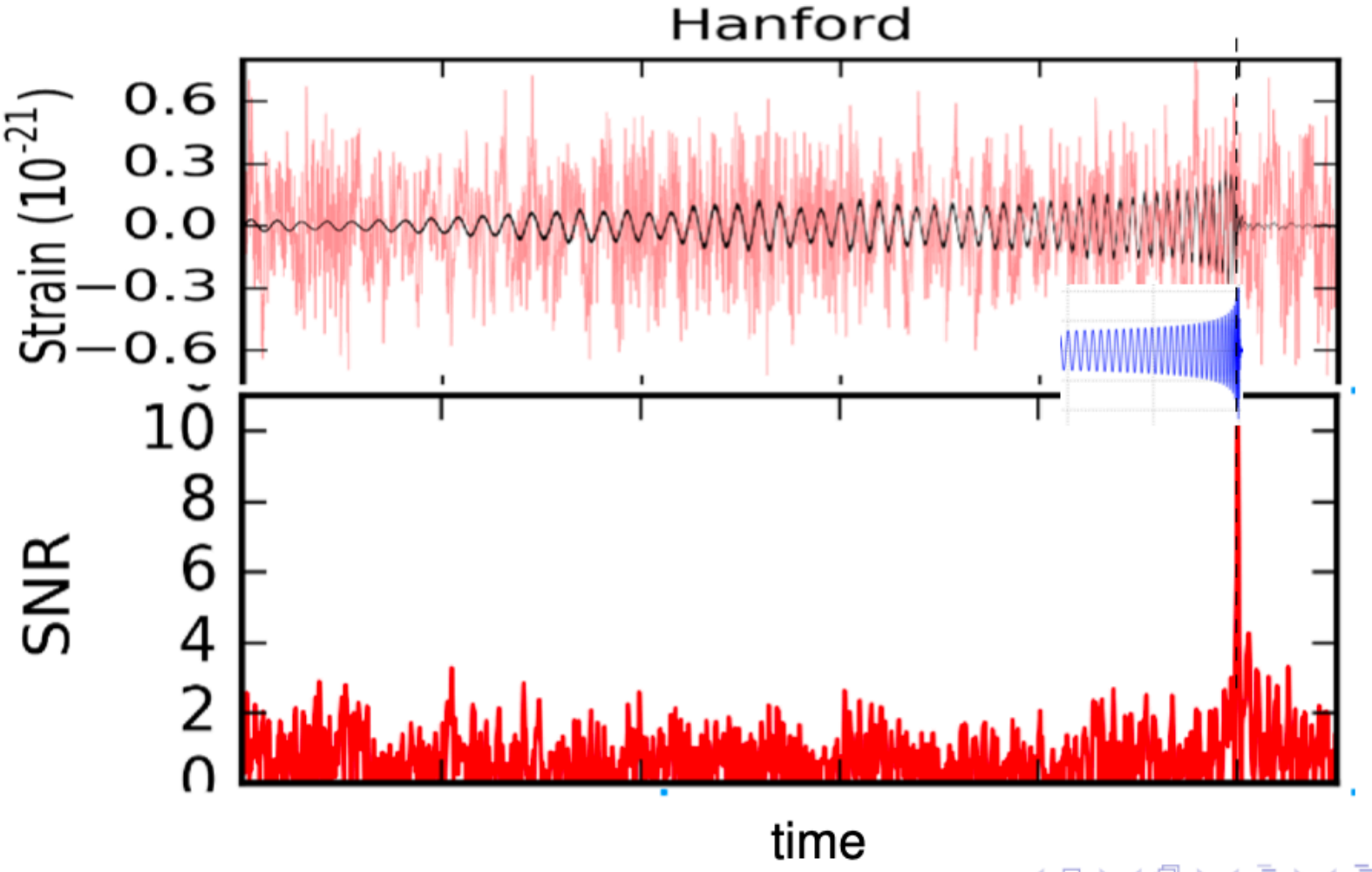

Matched filtering: GW150914

H1

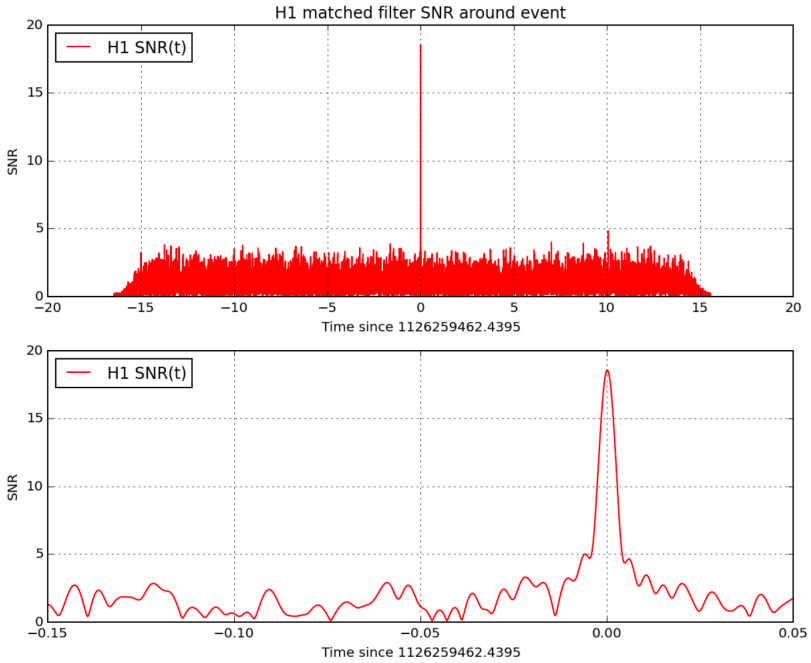

L1

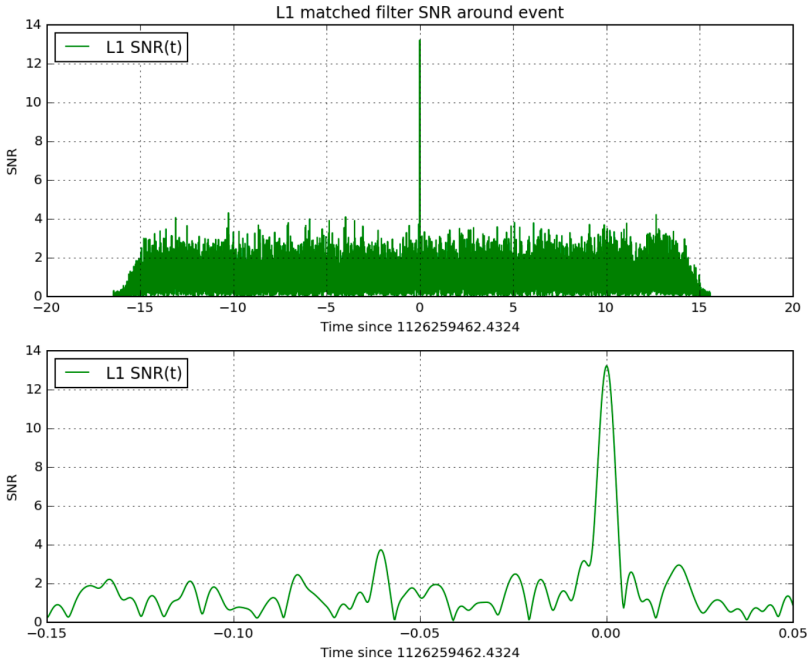

[LOSC: https://losc.ligo.org/tutorials/]

Template bank search

$$S(t) = 4 \int_{f_{low}}^{f_{final}} \frac{\tilde{d}(f)\,\tilde{T}^{*}(f)}{S_n(f)} e^{2\pi i f t}\, df$$

•Request Minimum Match = 0.97

⇒ Low Mass region is more densely populated than high mass region

GW150914: 250000 templates
(mass1, mass2, spin1, spin2)

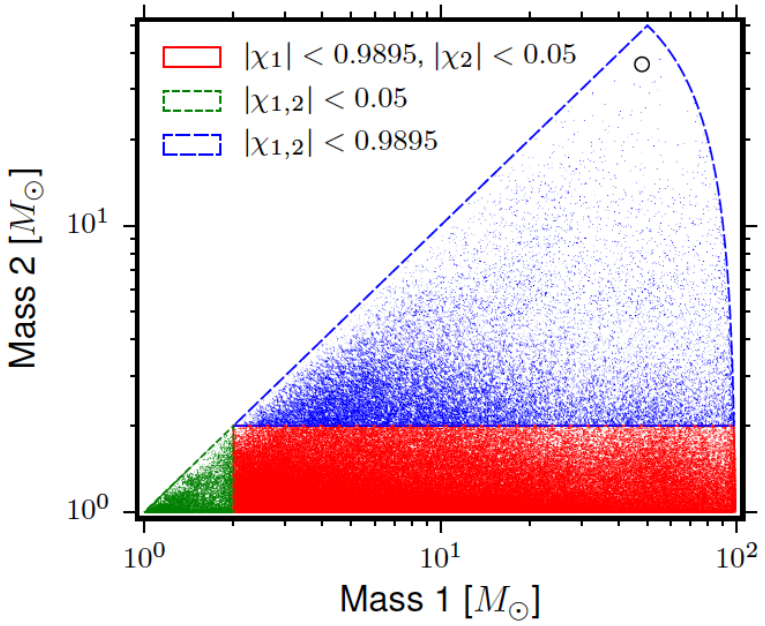

==> needs many computers for fast search

Parameter estimation

- Detection pipeline identifies the GW event.
- We want to know the physical parameters of the source.
- Once a detection is made, parameter estimation analysis is implemented.
- PE pipeline explores the whole parameter space.
- Number of parameters (BBH): 9 for nonspinning, 12 for one spinning, 15 for two spinning.

Matched filtering and parameter estimation: GW150914

H1

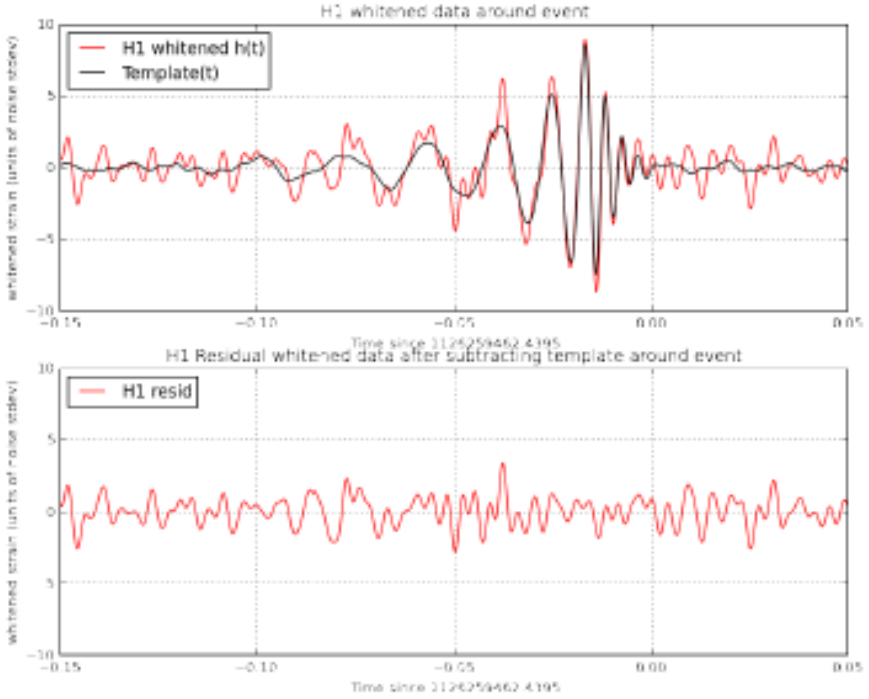

L1

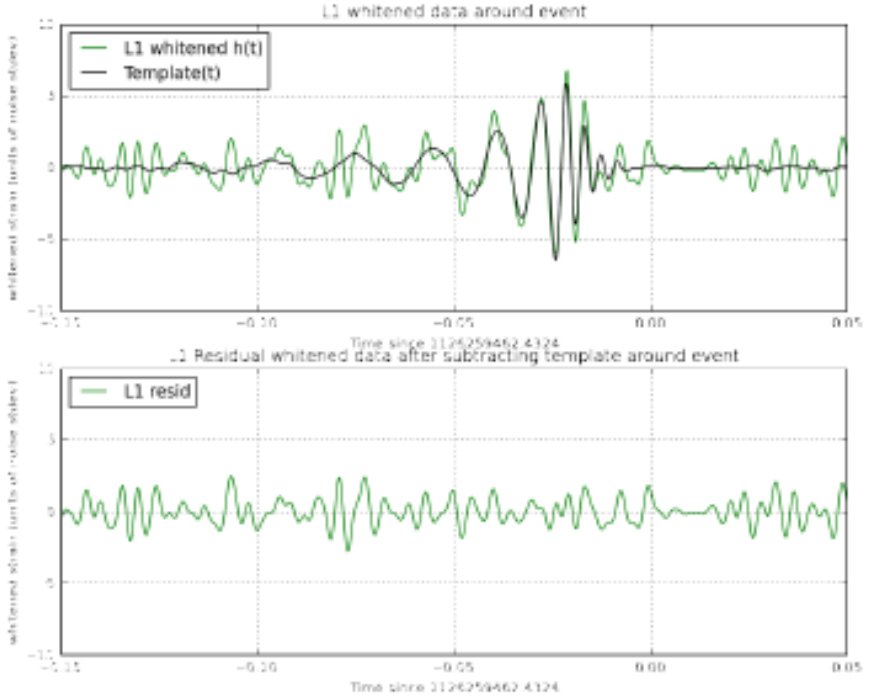

[LOSC: https://losc.ligo.org/tutorials/]

noise = data - signal

p(signal parameters)

= p(noise residuals)

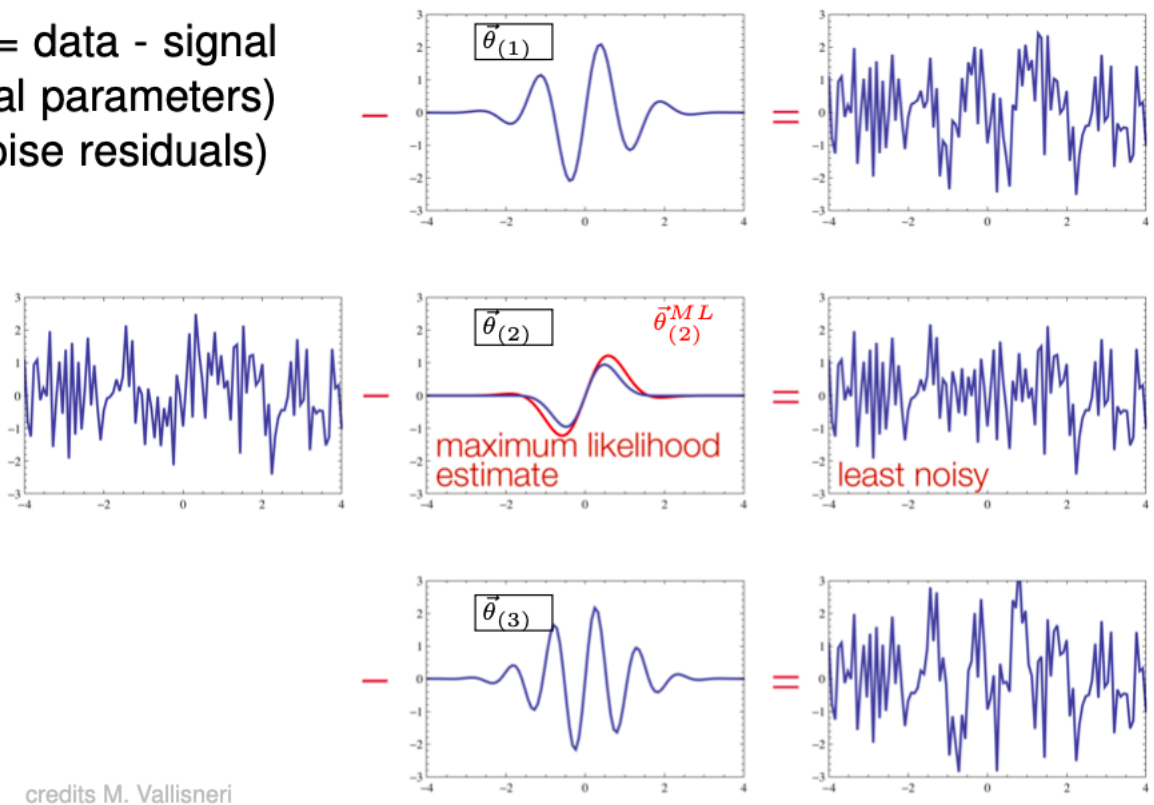

credits M. Vallisneri

Overlap: Parameter estimation

$$\langle x|h\rangle = 4\mathrm{Re}\int_0^\infty \frac{\tilde{x}(f)\tilde{h}^*(f)}{S_n(f)}df,$$ match (same as in detection)

$$p(\theta|x) \propto p(\theta)L(x|\theta).$$ Bayesian

posterior prior likelihood

$$L(x|\theta) \propto \exp\left[-\frac{1}{2}\langle x-h(\theta)|x-h(\theta)\rangle\right]$$ data - model waveform

$$= \exp\left[-\frac{1}{2}\langle s+n-h(\theta)|s+n-h(\theta)\rangle\right].$$

$$L(\theta) \propto \exp\left[-\frac{1}{2}\{\langle s|s\rangle + \langle h(\theta)|h(\theta)\rangle - 2\langle s|h(\theta)\rangle\}\right].$$ high SNR limits

$$L(\theta) \propto \exp[-\rho^2\{1-\langle \hat{s}|\hat{h}(\theta)\rangle\}],$$ match (overlap) btw hidden signal and model wfs

$\rho = \sqrt{\langle s|s\rangle}$ SNR

$\hat{h} \equiv h/\rho,$ normalized wf

Overlap: Parameter estimation pipeline

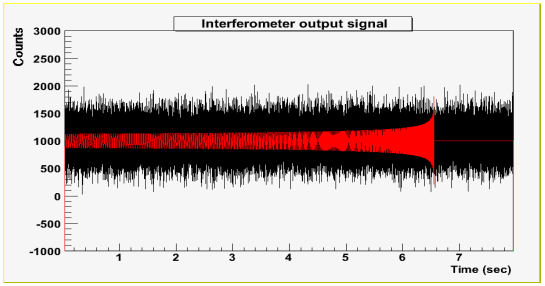

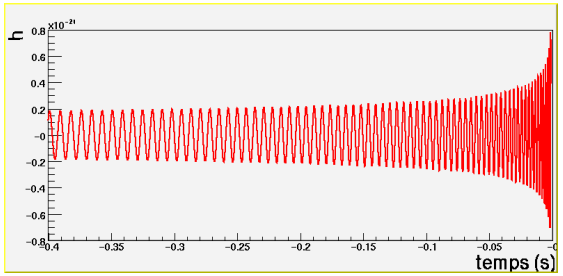

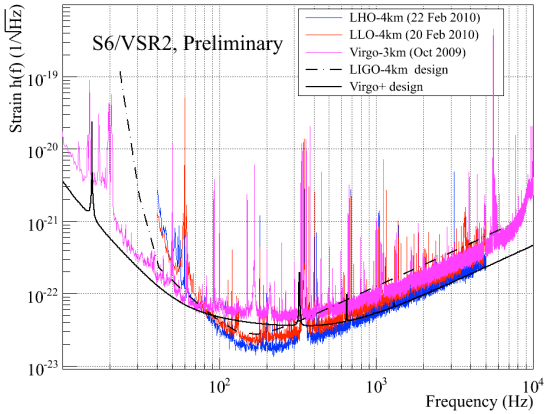

$$\langle d|T\rangle = 4Re\int_{f_{lower}}^{f_{final}} \frac{d(f)T^*(f)}{S_n(f)}df$$

$T(m_1, m_2, a_1, a_2, D, RA, Dec, ...)$ ==> **9~15 parameters**

- Template bank-based analysis is not possible
- Over 10^6 overlaps varying parameters
- Very long computation time
- PE result is given by posterior PDFs

Posterior example : NS-NS binary

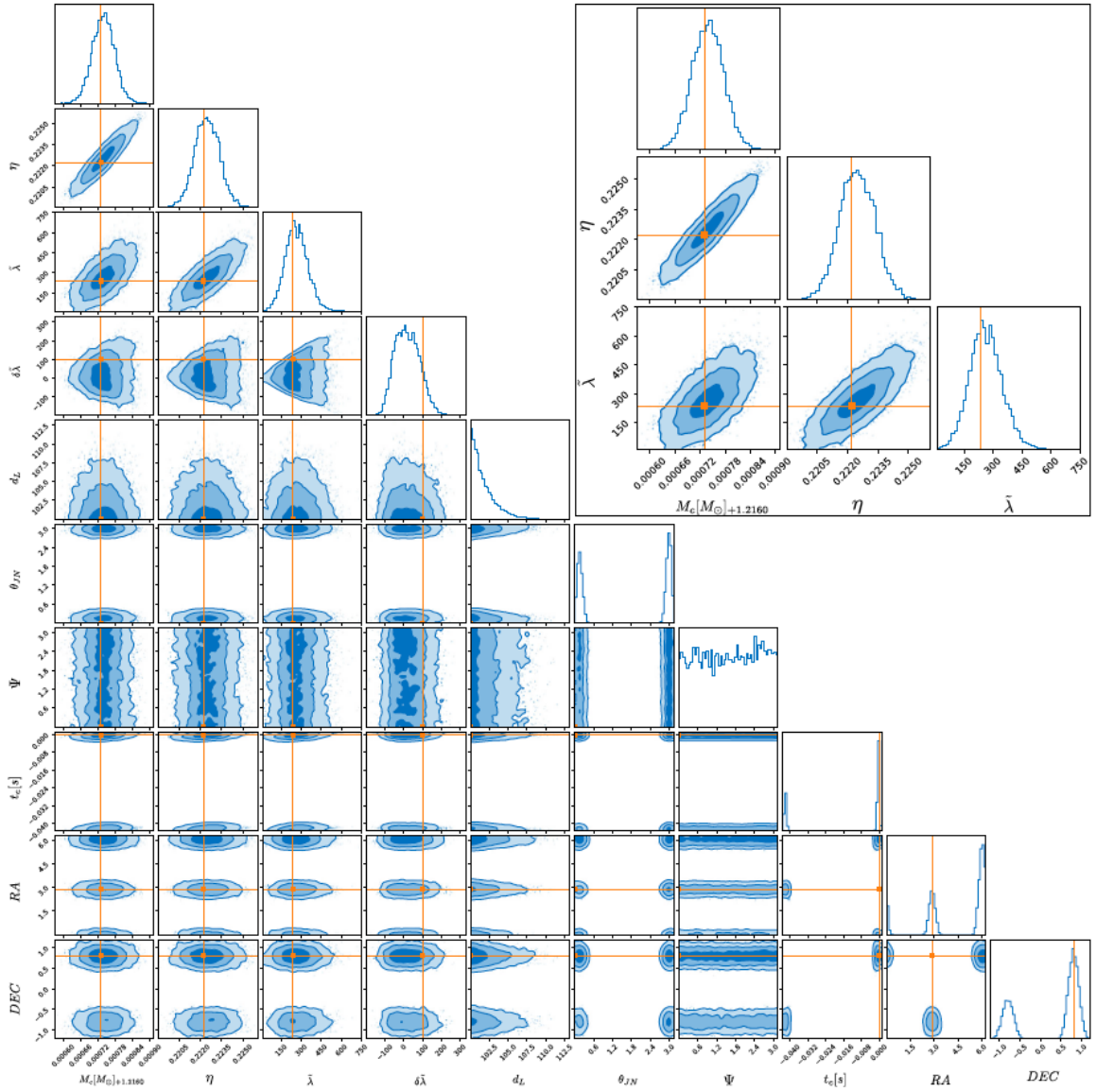

FIG. 16. Parameter estimation result for the same BNS source as in Fig. 1 with $\rho = 34$. We use the entire 11 parameters including the 5 extrinsic parameters. The zoom-in view of the posteriors for the three main parameters M_c, η, and $\tilde{\lambda}$ is given in the inset. ϕ_c was automatically marginalized and thus is not shown here. True values are marked in orange.

Impact of prior (GW170817)

$$p(\theta|x) \propto p(\theta)L(x|\theta).$$

posterior prior likelihood

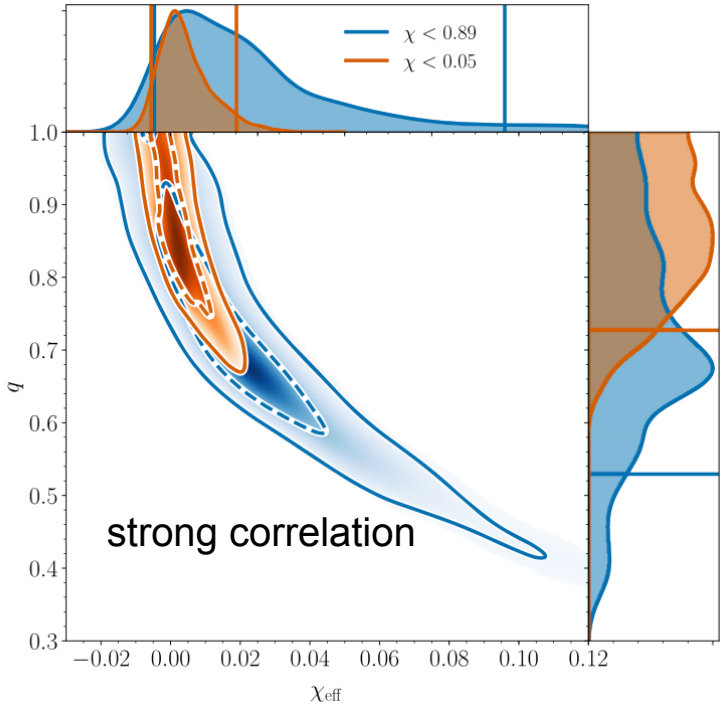

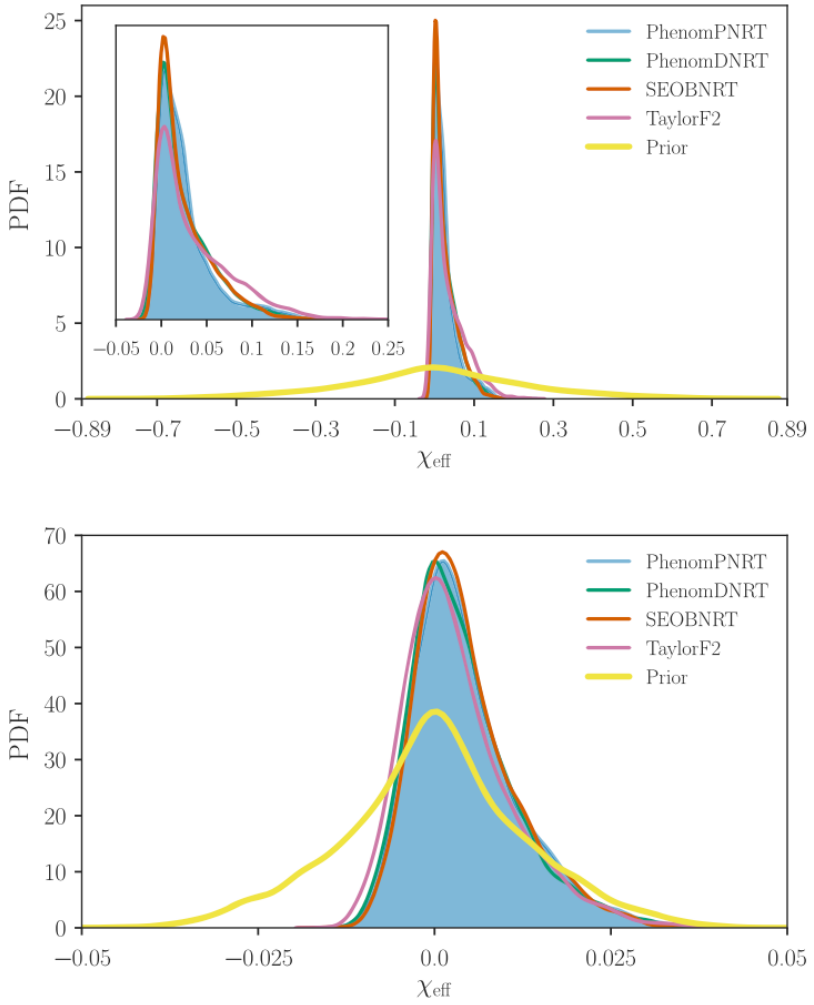

FIG. 6. Posterior PDF for the effective spin parameter $\chi_{\rm eff}$ using the high-spin prior (top panel) and low-spin prior (bottom panel). The four waveform models used are TaylorF2, PhenomDNRT, PhenomPNRT, and SEOBNRT.

Parameter estimation study

- PE aims to find the parameters of the GW source quickly and accurately when a real GW is detected.

- PE study using injection signals
- waveform models
- source parameters- mass, spin, NS tides, eccentricity, ..

- Two types of PE errors:

1) statistical uncertainty (measurement errors)
2) systematic error (systematic bias)

Measurement error

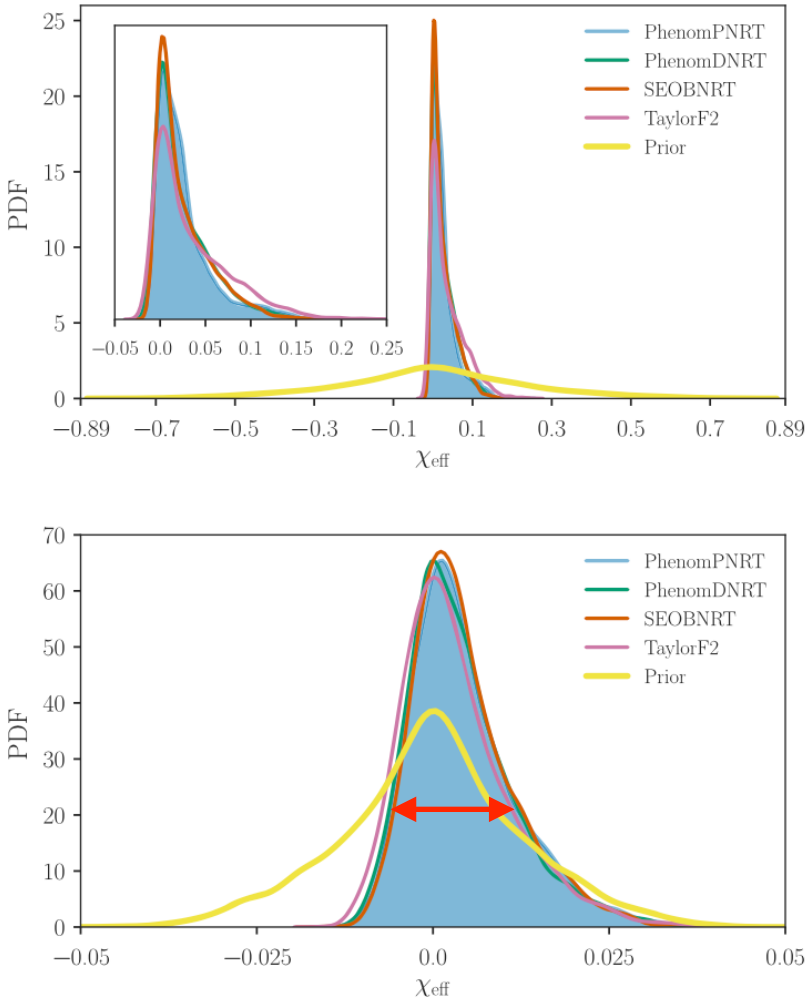

FIG. 6. Posterior PDF for the effective spin parameter $\chi_{\rm eff}$ using the high-spin prior (top panel) and low-spin prior (bottom panel). The four waveform models used are TaylorF2, PhenomDNRT, PhenomPNRT, and SEOBNRT.

confidence interval:
68%, 90%, 99%, ..

depends on
- prior
- SNR
  - source distance
  - detector sensitivity

Systematic bias

- If the template model is complete, recovered parameters are the same as the true values.
- If inaccurate model, recovered parameters are biased from the true values ==> systematic bias
- Ratio btw systematic bias and statistical error is important.
- Bias is independent of SNR, only depends on the model accuracy
- Injection study using various models

Outline

- Compact Binary Coalescence (CBC) waveforms
  - nonspinning
  - precessing (amplitude modulation)
  - PN phase evolution
  - waveform models
- CBC data analysis
  - matched filter
  - efficiency of template bank: fitting factor
  - detection & parameter estimation
- Systematic error in parameter estimation
  - examples
  - impact of eccentricity (review on recent works)

Example: spinning signal vs nonspinning template model

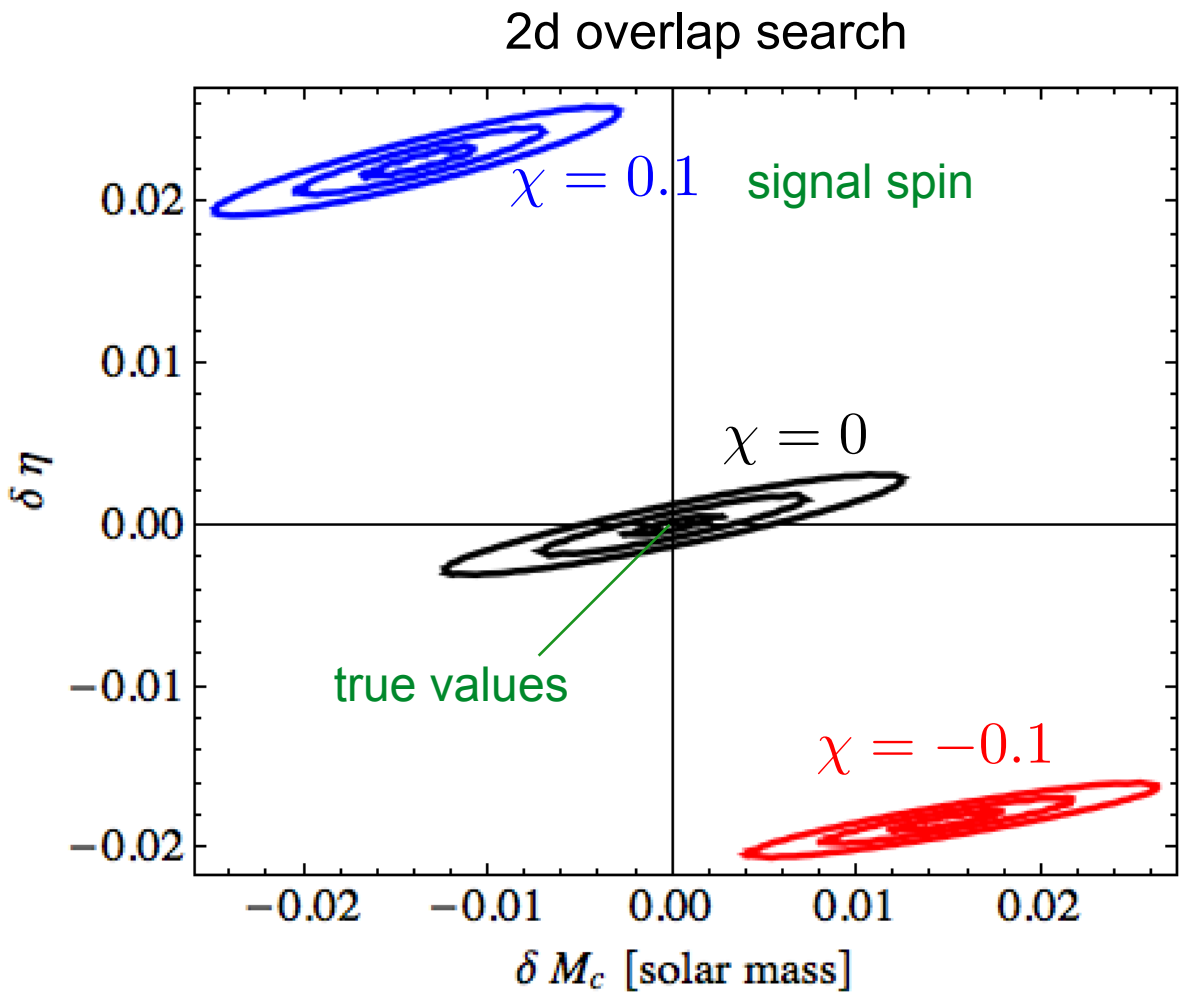

Bias

$$\eta^{\rm rec} < 0.25$$

$$M_c = \frac{(m_1 m_2)^{3/5}}{M^{1/5}}$$
$$\eta = \frac{m_1 m_2}{M^2}$$

$m_1/M_\odot$,	$m_2/M_\odot$
30,	5
50,	5
50,	10
70,	10
90,	10

Cho, PRD 94, 124045 (2016)

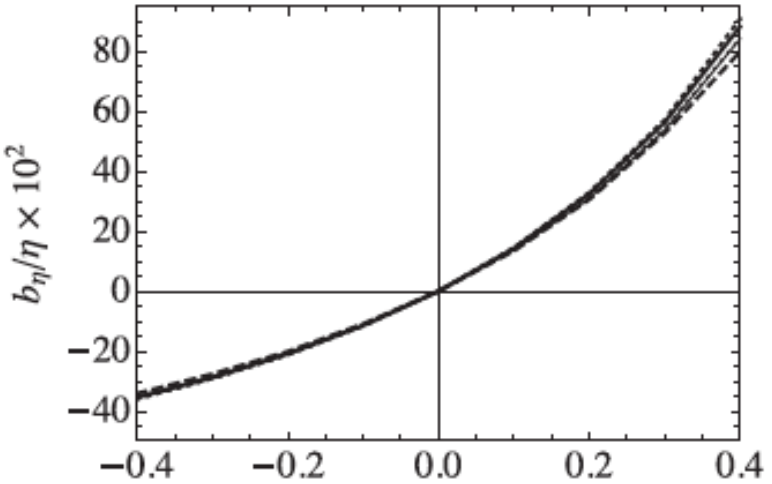

negative inclination

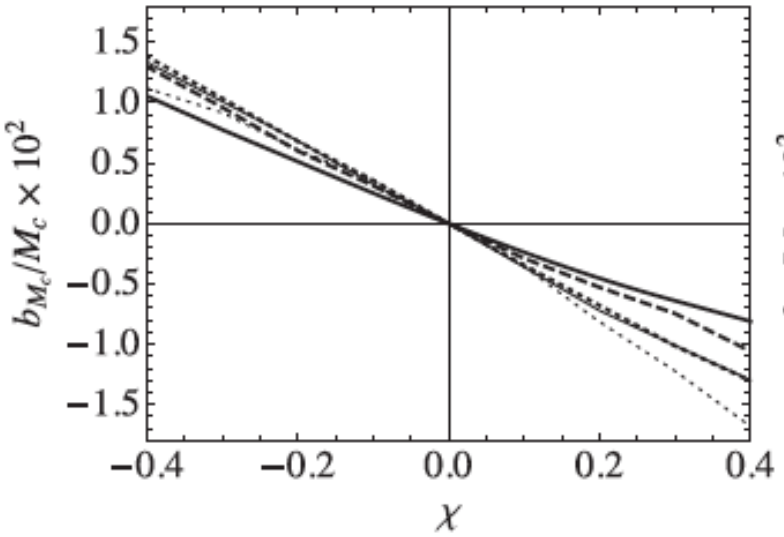

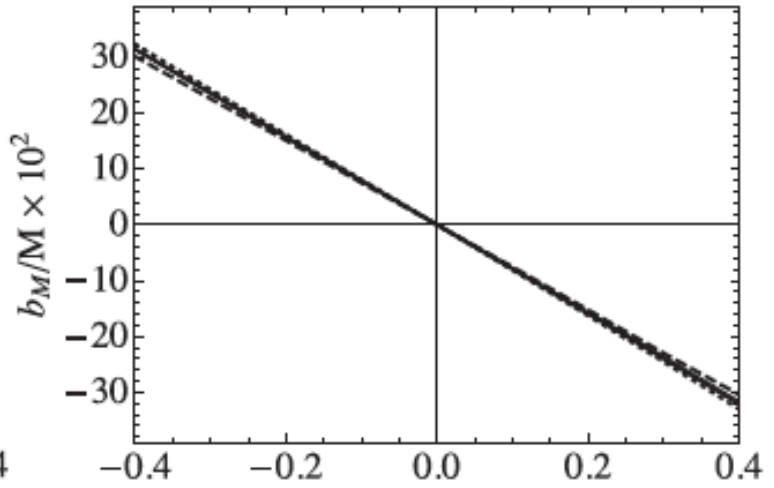

Spin effect vs mass effect

Binary dynamics		Wave function
aligned-spin spin-orbit coupling =>phase evolution slower =>longer waveform	⟷	less massive binary =>lower GW energy =>longer waveform
anti-aligned-spin spin-orbit coupling =>phase evolution faster =>shorter waveform	⟷	more massive binary =>higher GW energy =>shorter waveform

waveforms [f_{min}=30Hz]

$m_1 = m_2 = 10M_\odot$

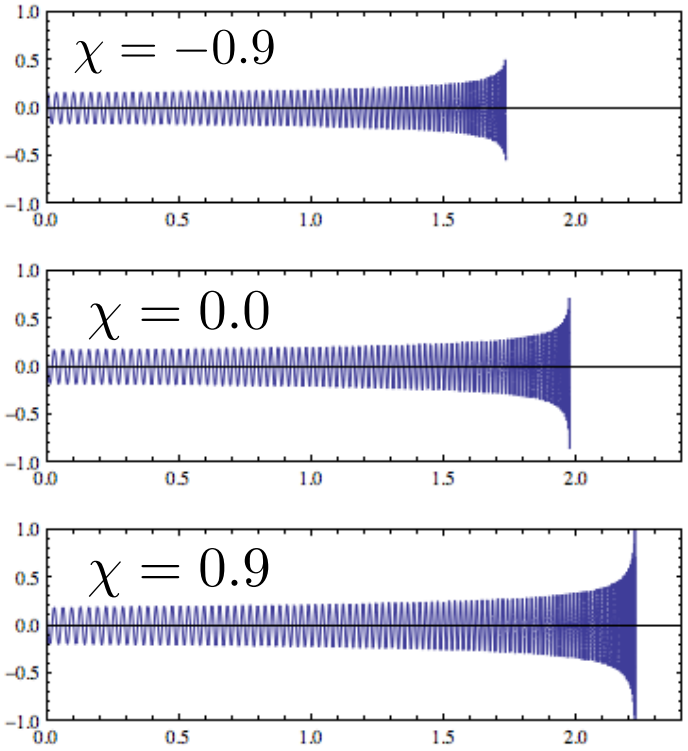

Time [s]

$\chi = 0.0$

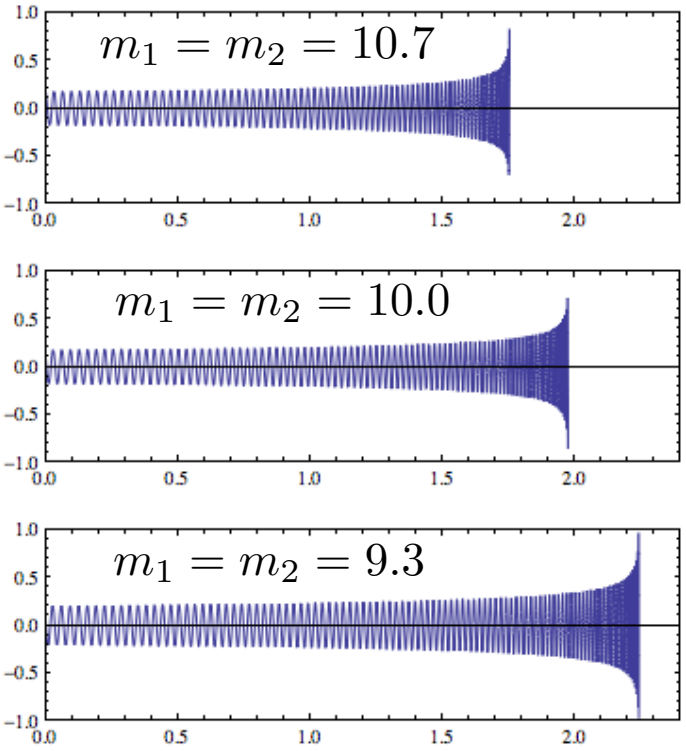

Time [s]

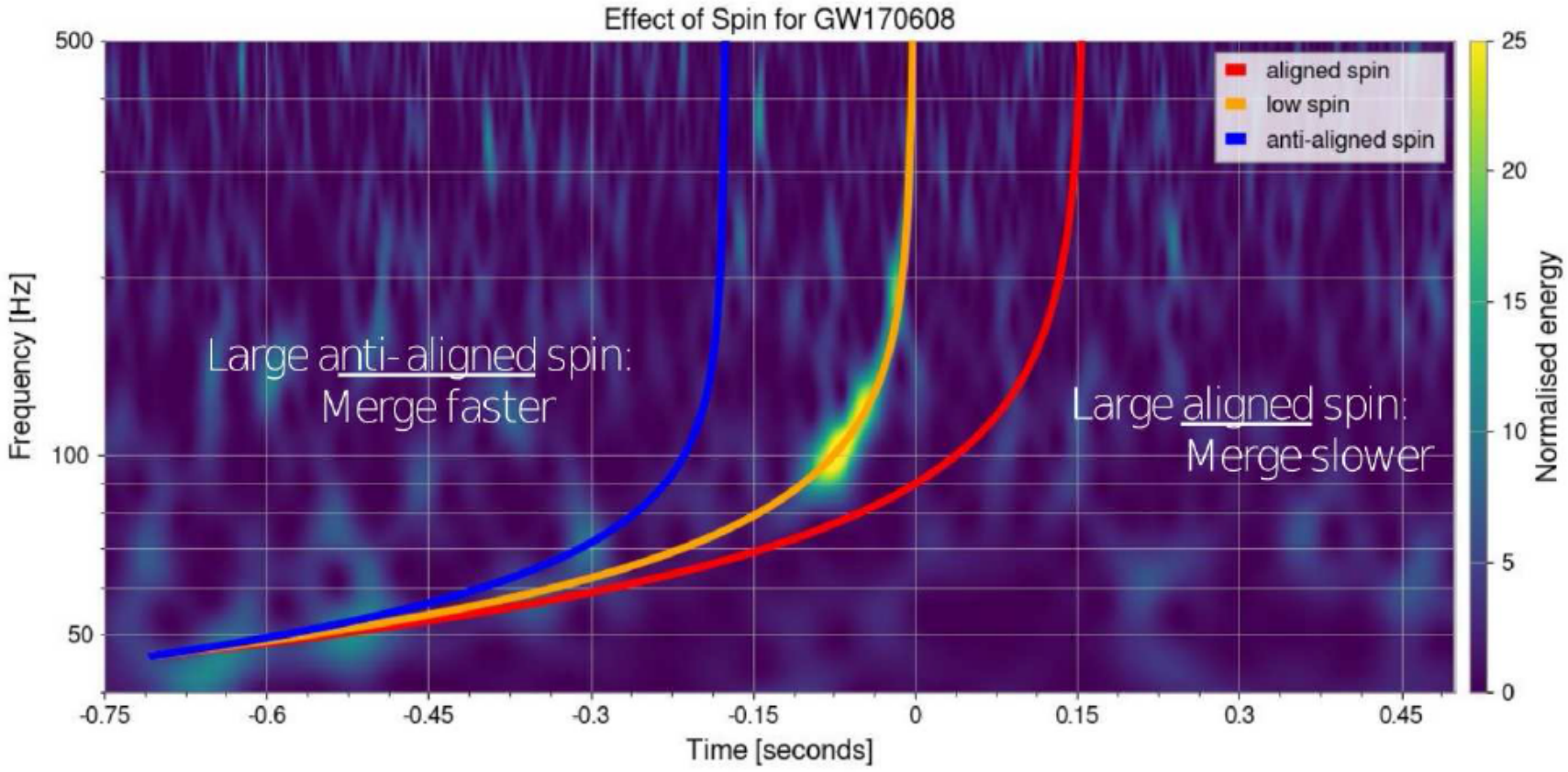

(see the pyCBC tutorial:
`http://pycbc.org/pycbc/latest/html/waveform.html#plotting-frequency-evolution-of-td-waveform`)

Result: bias vs. statistical error

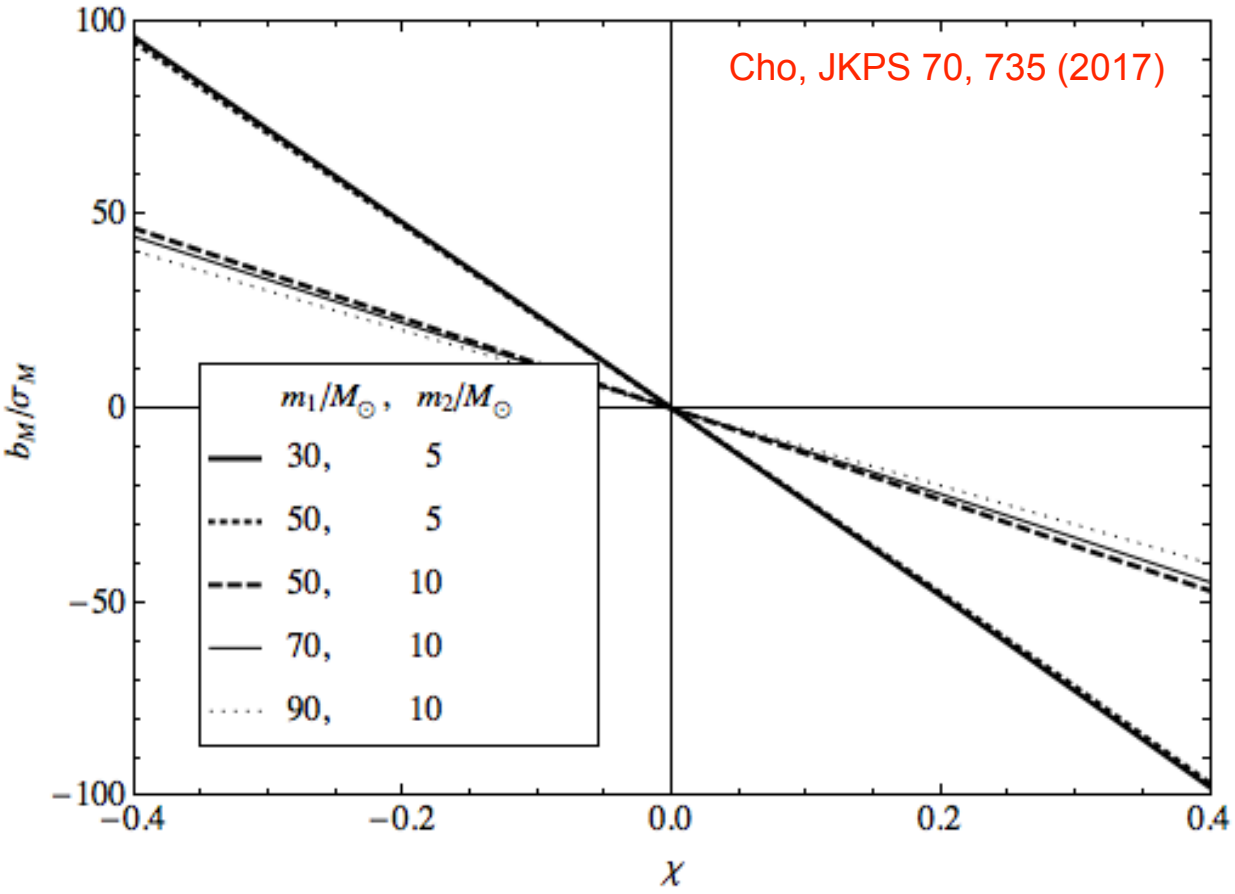

$$\sigma \ll b$$

SNR=20

$m_1[M_\odot]$, $m_2[M_\odot]$	30, 5	50, 5	50, 10	70, 10	90, 10
$\sigma_{M_c}/M_c \times 10^2$	0.065	0.110	0.250	0.359	0.520
$\sigma_\eta/\eta \times 10^2$	0.647	0.739	1.469	1.741	2.159
$\mathcal{C}_{M_c\eta}$	0.921	0.944	0.952	0.963	0.973
$\sigma_M/M \times 10^2$	0.329	0.341	0.648	0.705	0.798

Result: bias vs. statistical error

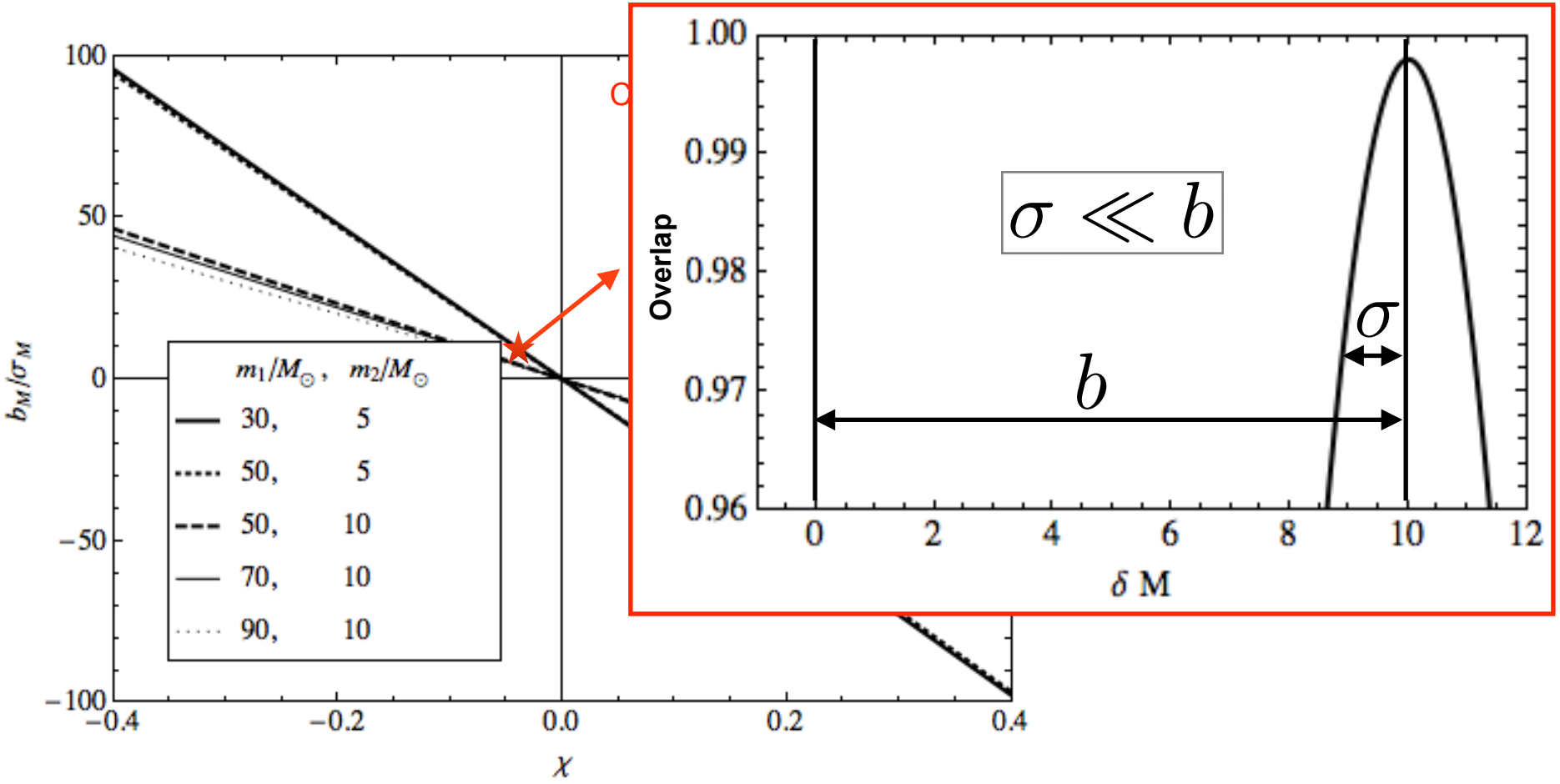

$m_1[M_\odot]$, $m_2[M_\odot]$	30, 5	50, 5	50, 10	70, 10	90, 10
$\sigma_{M_c}/M_c \times 10^2$	0.065	0.110	0.250	0.359	0.520
$\sigma_\eta/\eta \times 10^2$	0.647	0.739	1.469	1.741	2.159
$\mathcal{C}_{M_c\eta}$	0.921	0.944	0.952	0.963	0.973
$\sigma_M/M \times 10^2$	0.329	0.341	0.648	0.705	0.798

SNR=20

Bias due to eccentricity ?

GW151226-like BBH, nonspinning case

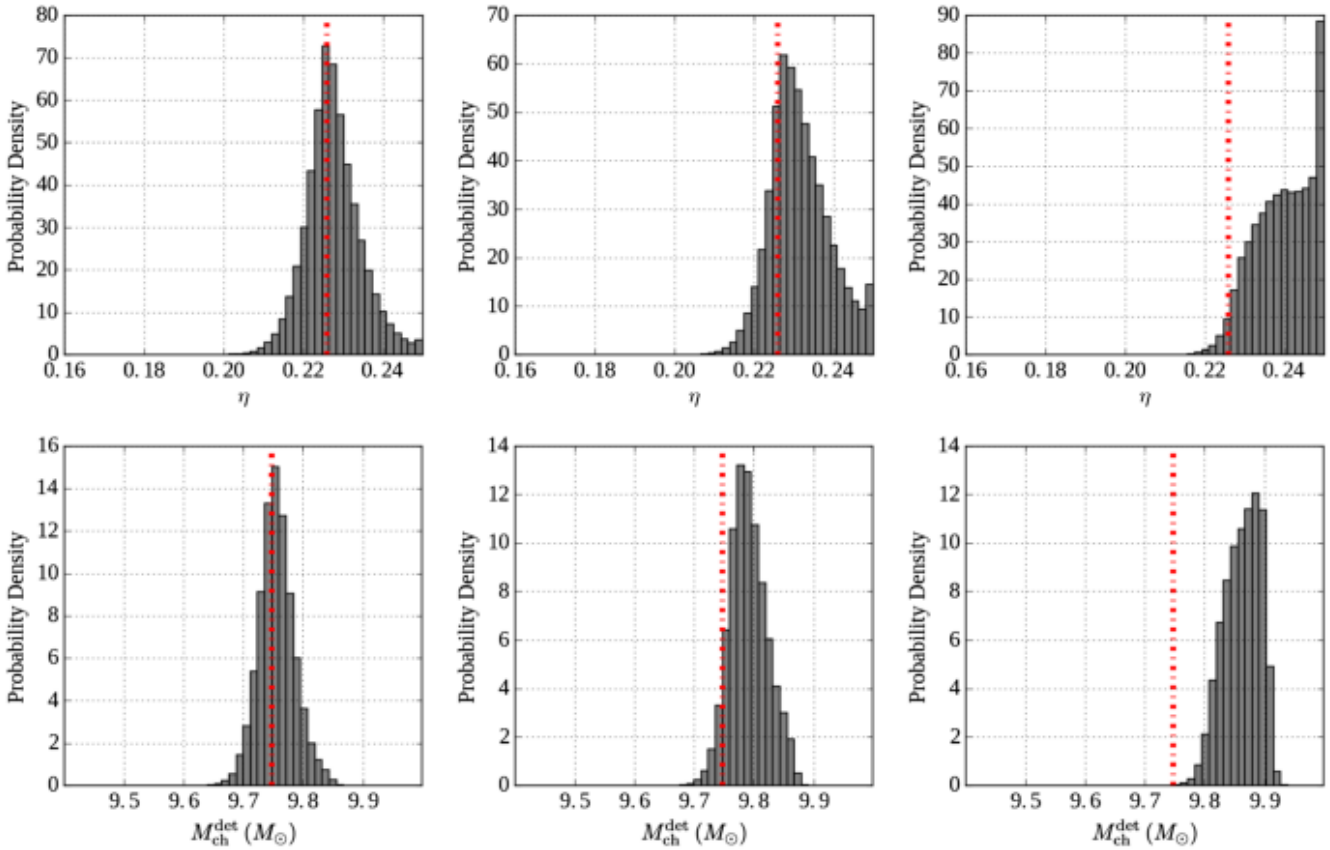

FIG. 7. Marginalized posterior probability distributions for the symmetric mass ratio η (top row) and the detector-frame chirp mass $M_{\rm ch}^{\rm det}$ (bottom row), showing the systematic bias induced by the signal's unmodeled eccentricity. Eccentric signals are injected with the `TaylorF2Ecc` waveform, but recovered using circular `TaylorF2` templates. As in Fig. 2, the vertical dotted lines indicate the injected values of η and $M_{\rm ch}^{\rm det}$ (which are the same in each row). The injected eccentricity varies as $e_0^{\rm inj} = [0.04, 0.12, 0.2]$ from left to right. A growing systematic bias is clearly seen as the eccentricity increases.

PRD 105, 023003 (2022) Favata et al.

signal: inspiral, nonspinning, eccentric BBH

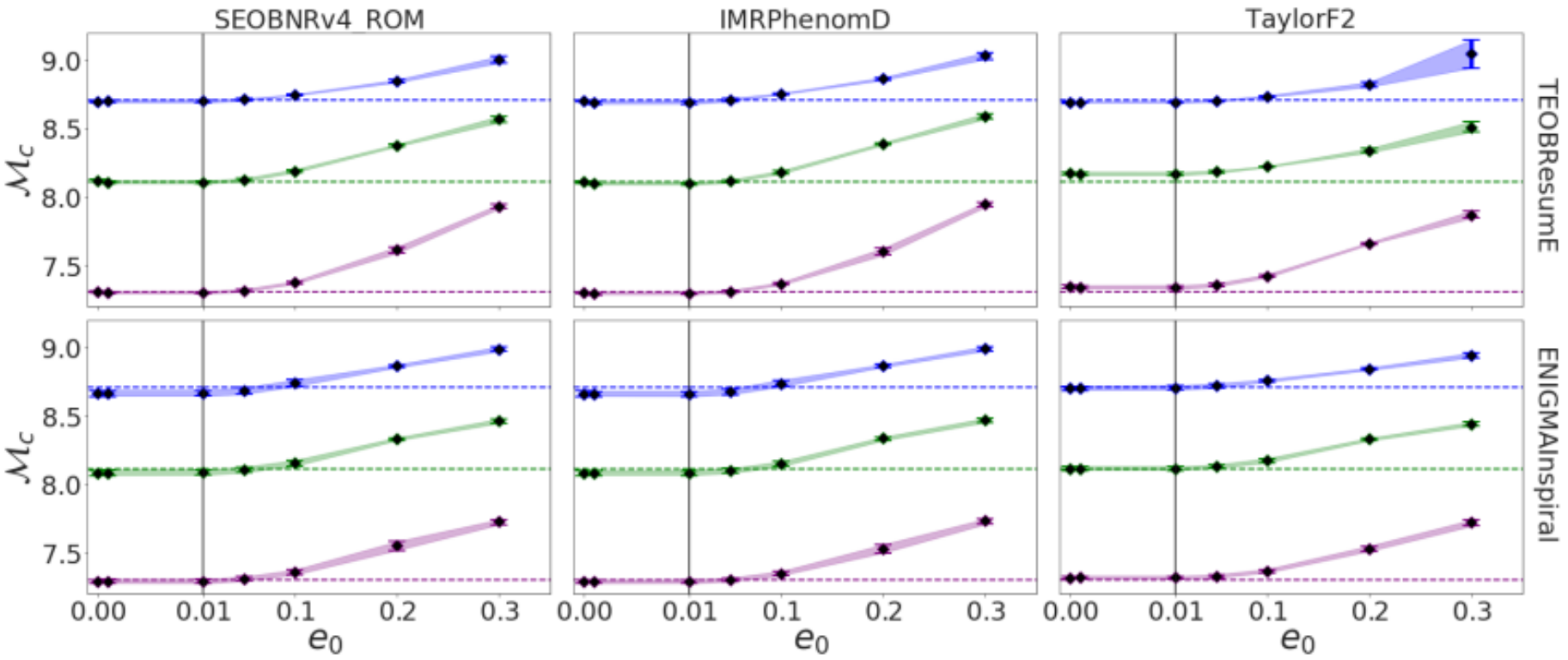

FIG. 3. Estimated values of the chirp mass for signals at different eccentricities. Dashed lines indicate the value of the simulated signal. The colors blue, green and purple correspond to the $q = 1, 0.5, 0.33$ signals respectively. The bars represent the 90% confidence intervals, with the diamond representing the median value. The shaded connects the ends of the error bars to illustrate the upward trend. The labels on top specify which model was used in the parameter estimation, and the labels on the right side of the figure specify which model was used to simulate the signal. Note the different scales between $[0., 0.01]$ and $[0.01, 0.3]$ on the x-axes.

arXiv:2107.07981

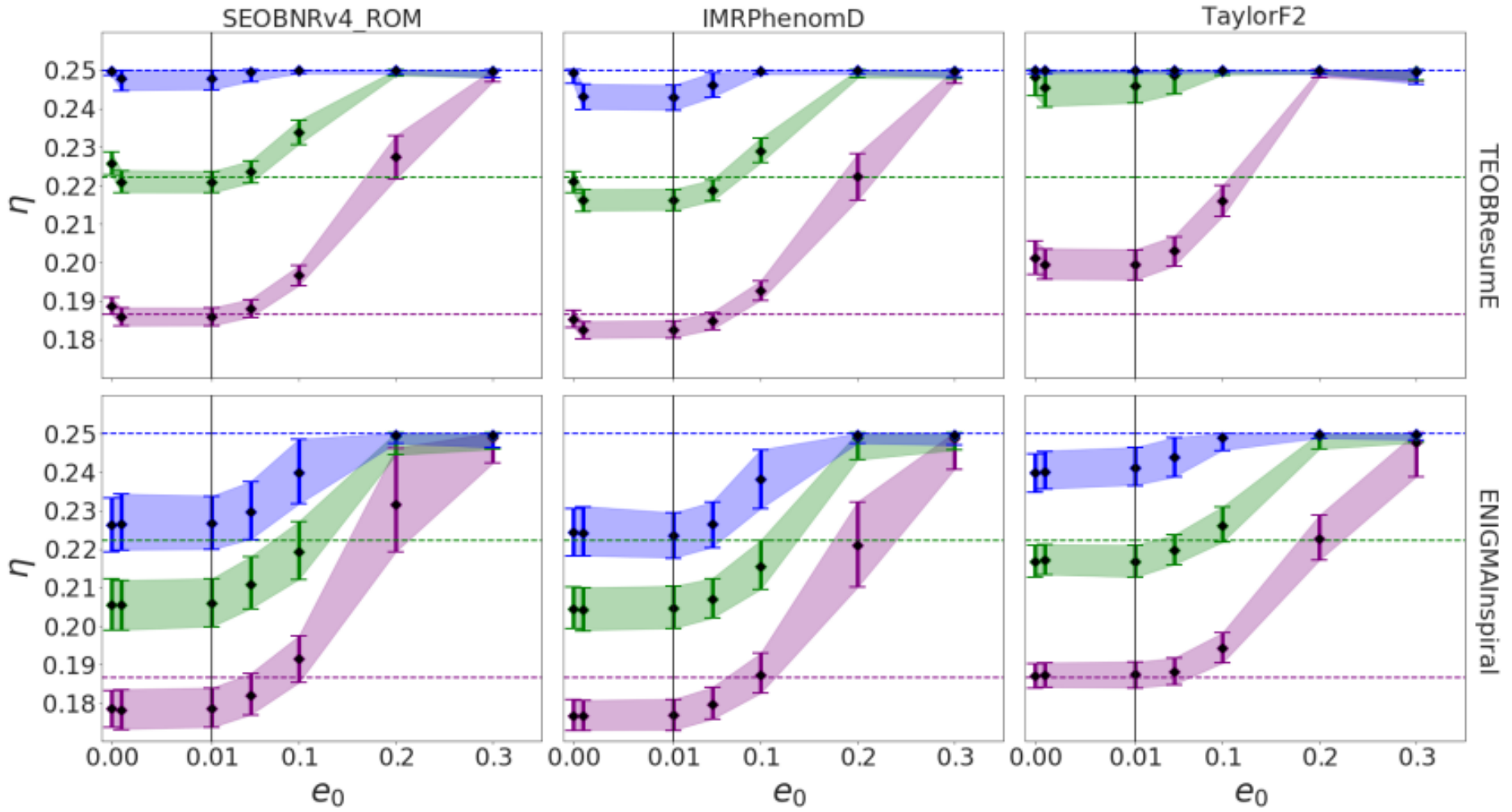
SEOBNRv4_ROM
IMRPhenomD
TaylorF2
TEOBResumE
ENIGMAInspiral
η
e_0
0.25
0.24
0.23
0.22
0.21
0.20
0.19
0.18
0.00
0.01
0.1
0.2
0.3

NS-NS binary ?

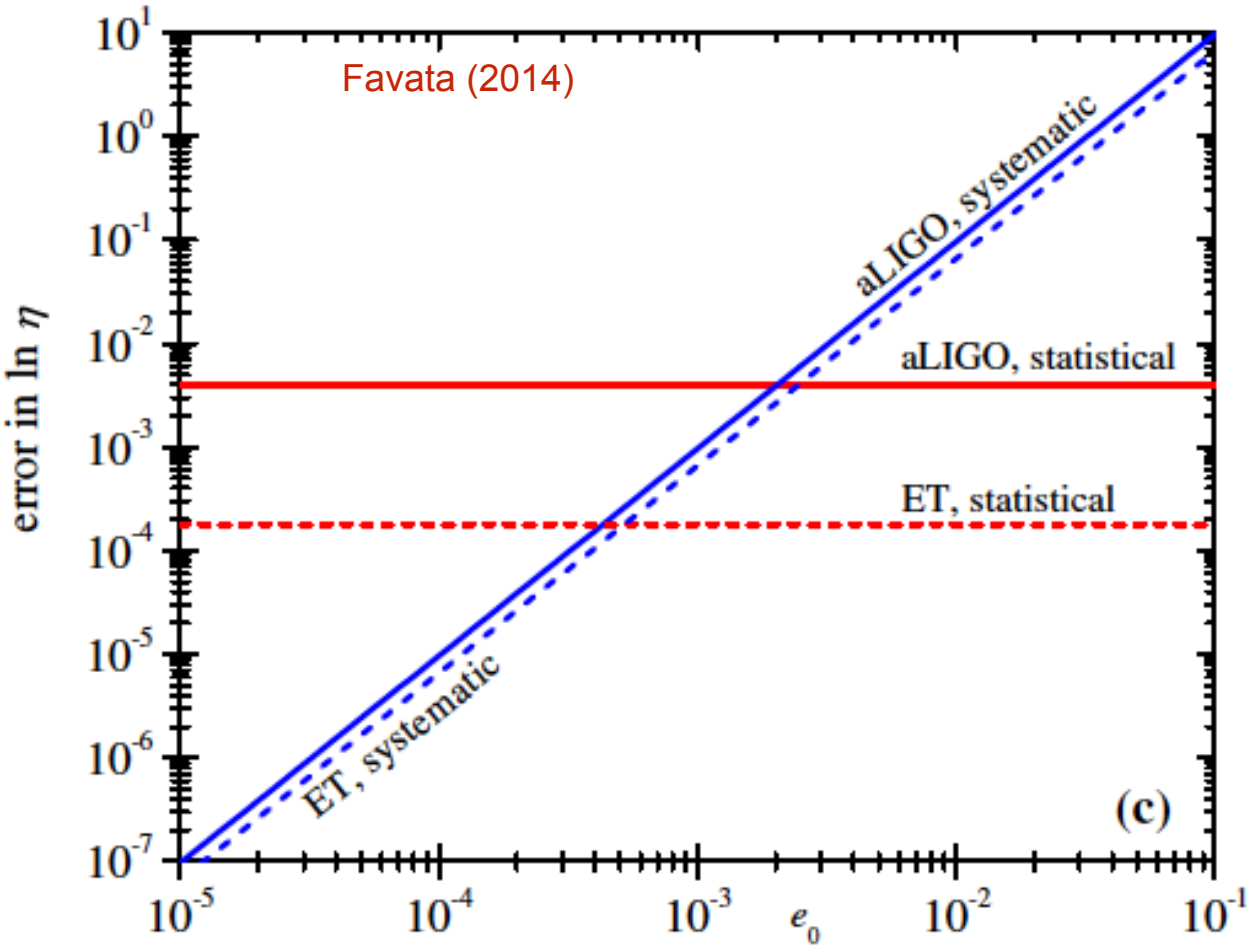

Fisher-Cutler-Vallisneri (FCV) methods,

Fisher-Cutler-Vallisneri (FCV) methods,

$$\Delta\theta_i = \theta_i^{\rm rec} - \theta_{i0} = \Sigma_{ij}(\partial_j h_{\rm AP}|h_{\rm T} - h_{\rm AP}),$$

h_T - true waveform

h_{AP} - approximate waveform

$\Sigma_{ij} = \Gamma_{ij}^{-1}$ using h_{AP}

Analytic method so fast and easy to use

but

high SNR limit (FM based),

small difference ($h_T - h_{AP}$)

validity unknown

Systematic bias due to eccentricity in parameter estimation for merging binary neutron stars

eccentric signal vs. circular template ==> bias ?

Bayesian PE vs. FCV

$$h(f) = \frac{M_c^{5/6}}{\pi^{2/3} D_{\rm eff}} \sqrt{\frac{5}{24}} f^{-7/6} e^{i\Psi(f)},$$

TaylorF2Ecc

$$\Psi(f) = 2\pi f t_c - 2\phi_c - \frac{\pi}{4} + \frac{3}{128\eta v^5}[\phi^{\rm pp,circ}(f) + \phi^{\rm tidal}(f) + \phi^{\rm ecc}(f)],$$

phase (nonspinning)

$$\phi^{\rm Tidal} = -\left[\frac{39\tilde{\lambda}}{2} v^{10} + \left(\frac{3115\tilde{\lambda}}{64} - \frac{6595\sqrt{1-4\eta}\delta\tilde{\lambda}}{364}\right) v^{12}\right].$$

tidal correction

$$\phi^{\rm ecc} = -\frac{2355}{1462} e_0^2 \left(\frac{v_0}{v}\right)^{19/3} \left[1 + \left(\frac{18766963}{2927736}\eta + \frac{299076223}{81976608}\right) v^2 + \left(\frac{2833}{1008} - \frac{197}{36}\eta\right) v_0^2 + O(v^4) + \cdots + O(v^6)\right],$$

ecc. correction

Bayesian posterior

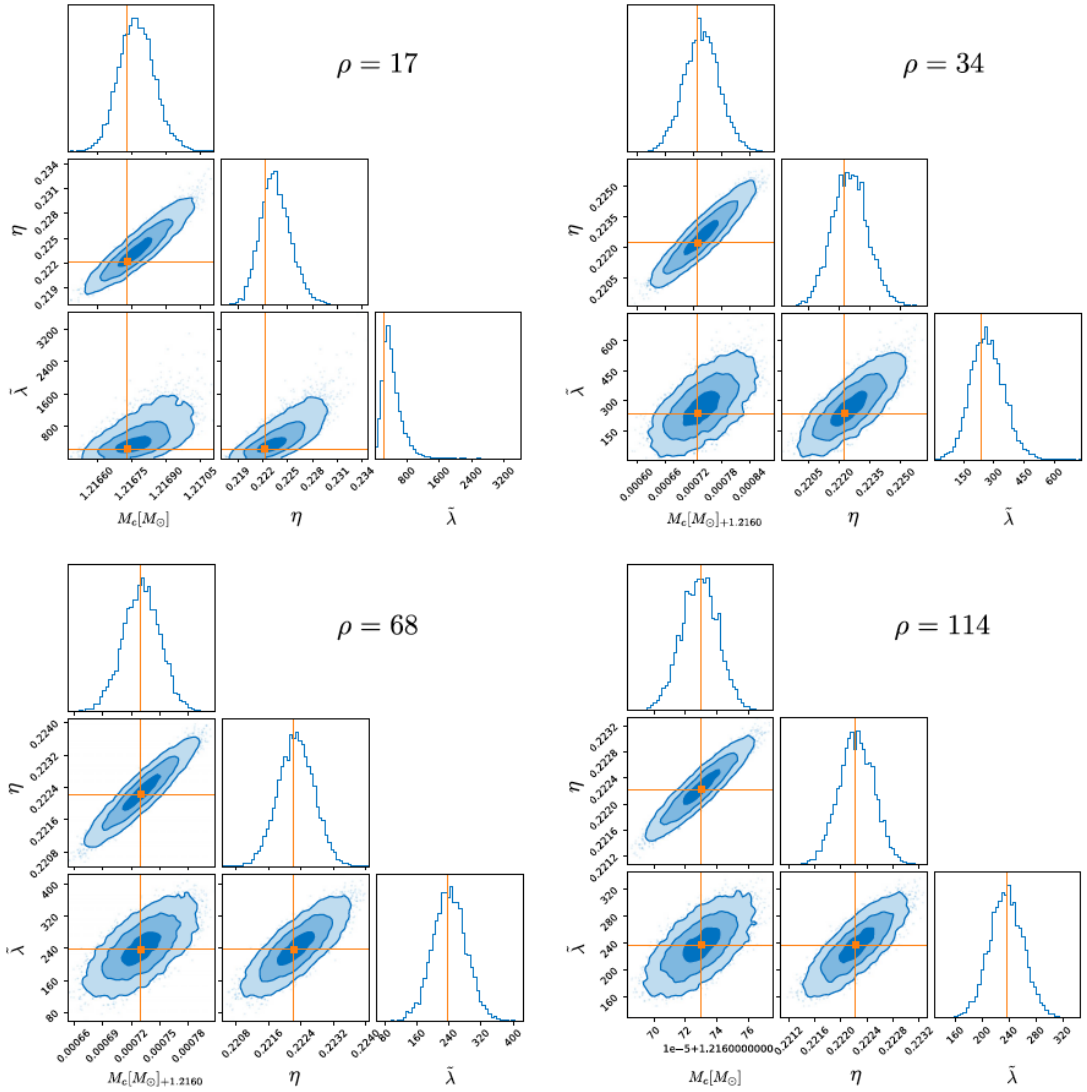

FIG. 1. Marginalized 1–d posterior PDF and 2–d confidence regions with the SNRs $\rho = 17$, 34, 68, and 114. The contours indicate 39, 86, and 99% confidence regions. Injection values are $(m_1, m_2, [M_c, \eta], \lambda_1, \lambda_2, [\tilde{\lambda}, \delta\tilde{\lambda}]) = (2M_\odot, 1M_\odot, [1.21673M_\odot, 0.22222], 14.7, 1744, [237, 101])$ marked in orange.

Bayesian vs. FM : measurement error

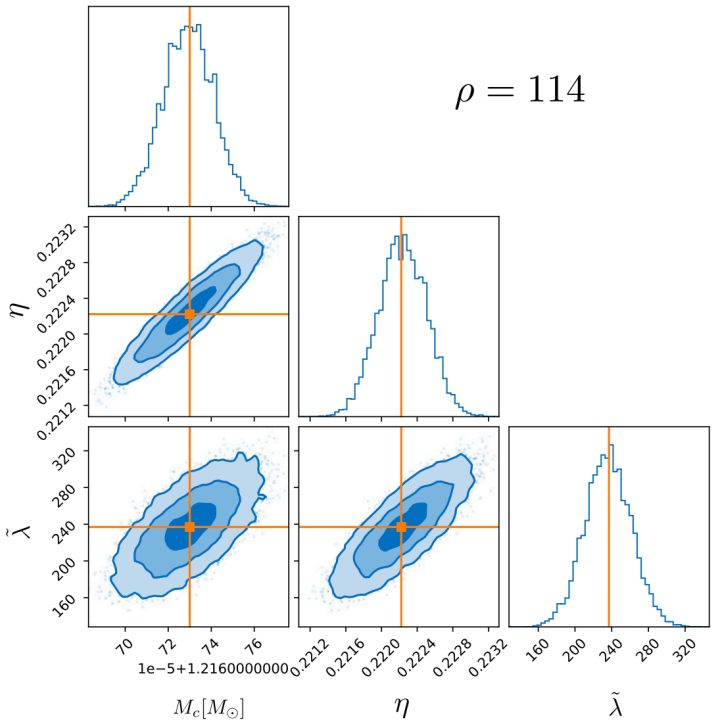

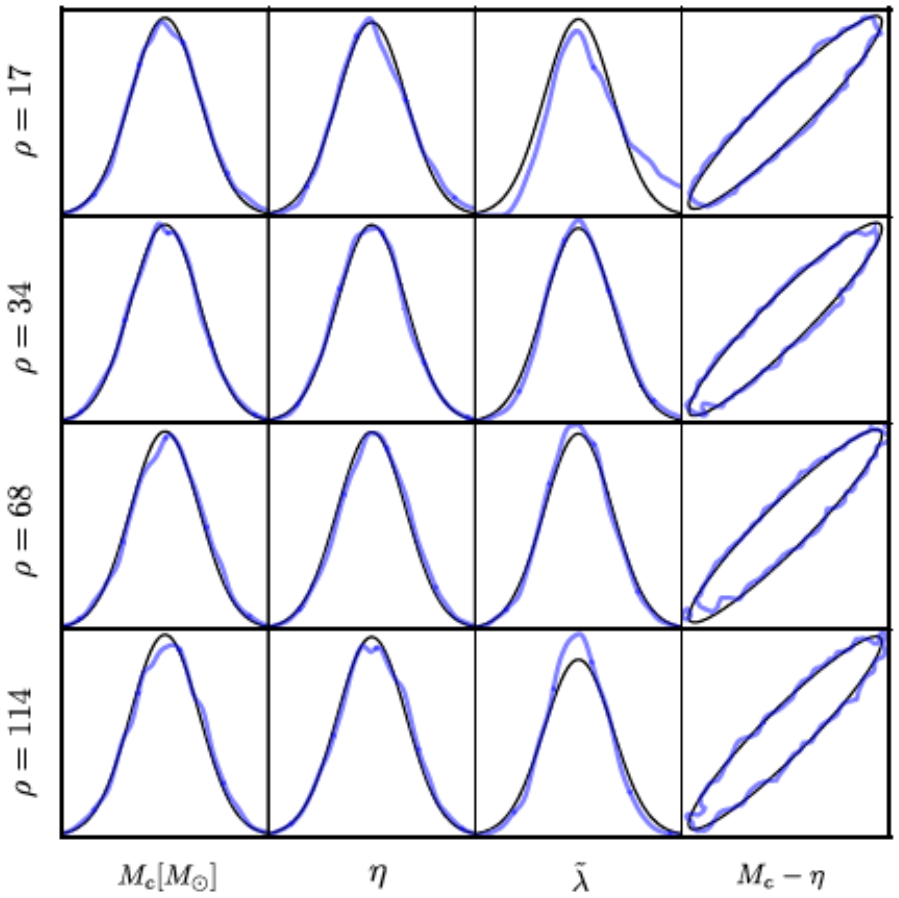

FM is well defined !

Bayesian vs. FVC : bias

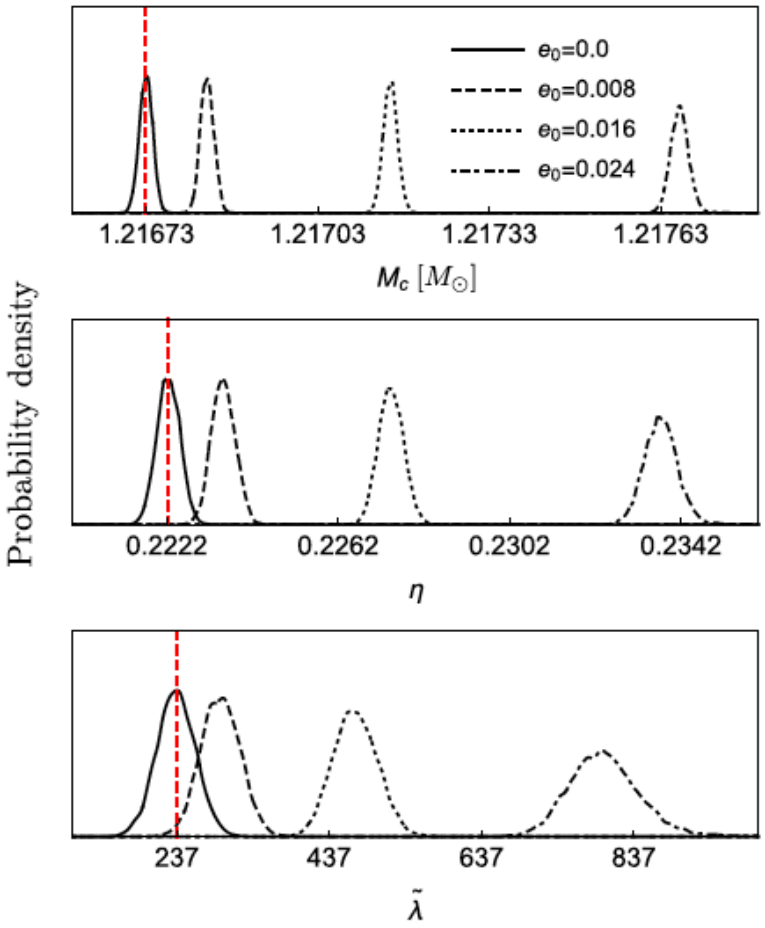

	Bayesian			FCV		
e_0	$\Delta M_c/\sigma_{M_c}$	$\Delta\eta/\sigma_\eta$	$\Delta\tilde{\lambda}/\sigma_{\tilde{\lambda}}$	$\Delta M_c/\sigma_{M_c}$	$\Delta\eta/\sigma_\eta$	$\Delta\tilde{\lambda}/\sigma_{\tilde{\lambda}}$
0.008	2.841	1.443	0.685	2.955	1.542	0.696
0.016	11.42	5.902	2.634	11.82	6.170	2.784
0.024	24.71	12.84	6.531	26.60	13.88	6.264

consistent

Bayesian vs. FVC : bias

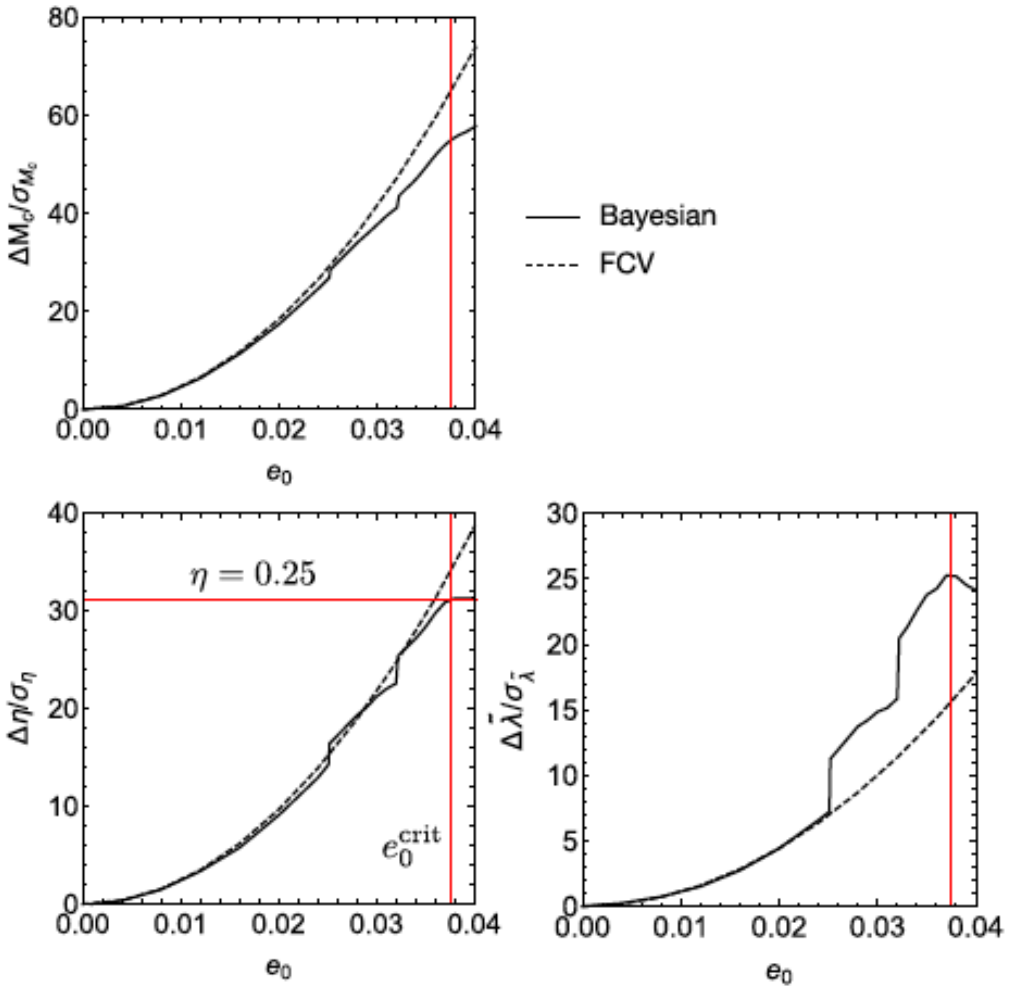

Bayesian vs. FVC : bias

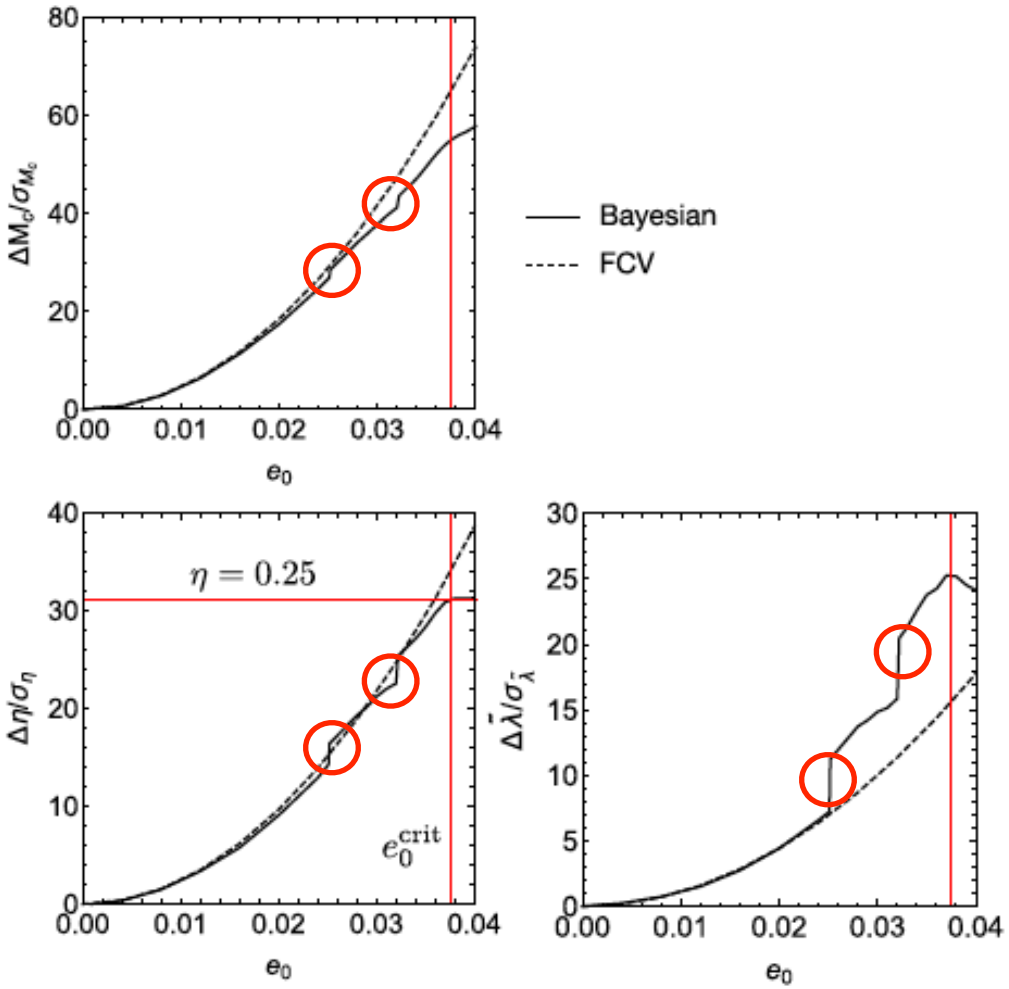

Bimodal !

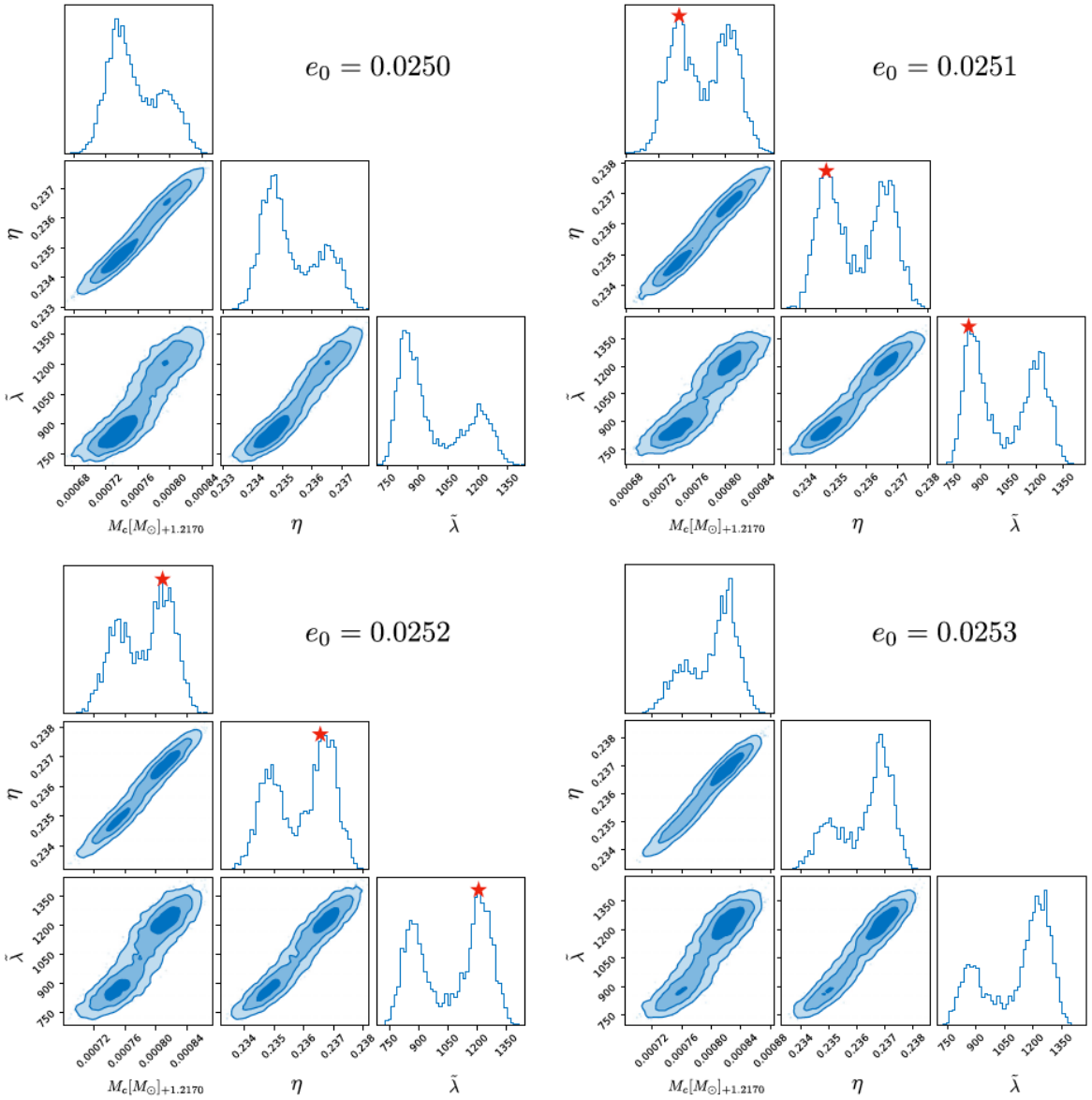
$e_0 = 0.0250$
$e_0 = 0.0251$
$e_0 = 0.0252$
$e_0 = 0.0253$
$M_c[M_\odot]_{+1.2170}$
η
$\tilde{\lambda}$

Monte Carlo study : FVC

10^4 Monte Carlo samples

4582 satisfy $\eta^{\rm rec} \leq 0.25$.

$1\ M_\odot \leq m_{1,2} \leq 2\ M_\odot (m_2 \leq m_1)$

$0 \leq e_0 \leq 0.025$.

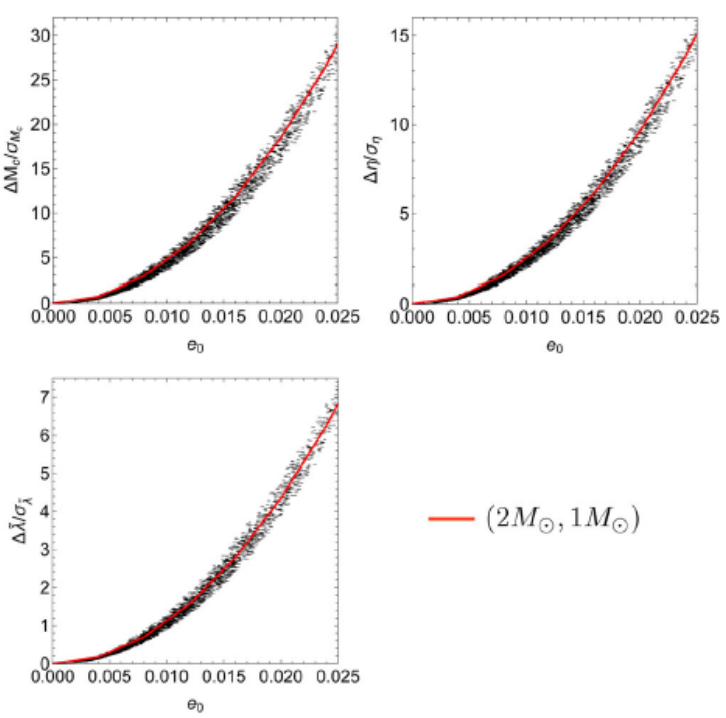

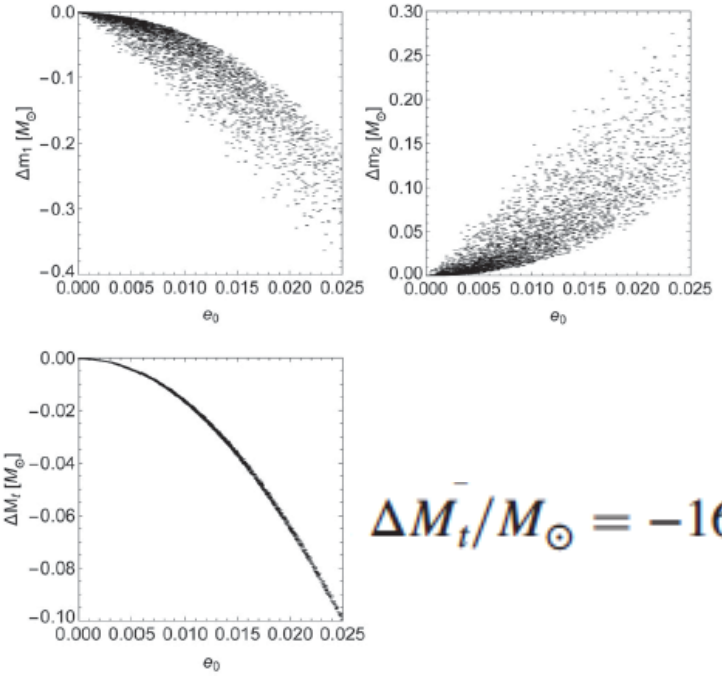

$$\Delta M_t/M_\odot = -160 e_0^2.$$

Injection study

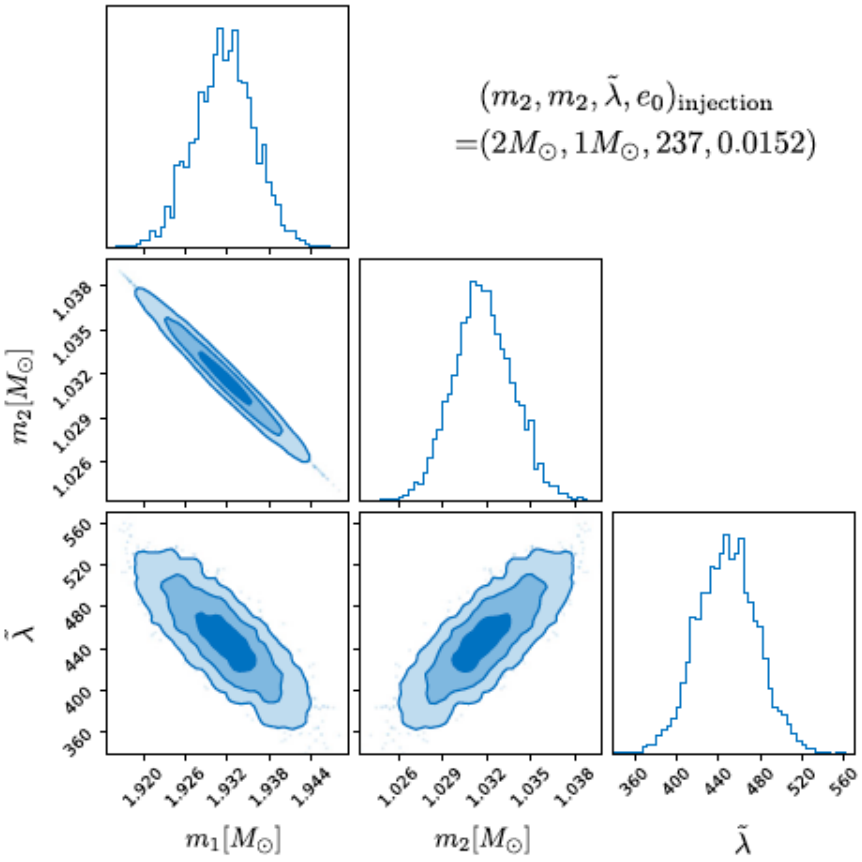

soft EOS with ecc. injection

but stiffer EOS PE result

Thanks !